

Modeling the transmission of new coronavirus in São Paulo State, Brazil – Assessing epidemiological impacts of isolating young and elder persons

Hyun Mo Yang^{1*}, Luis Pedro Lombardi Junior¹ and Ariana Campos Yang²

¹UNICAMP – IMECC – DMA; Praça Sérgio Buarque de Holanda, 651;
CEP: 13083-859, Campinas, SP, Brazil

²HC-FMUSP and HC-UNICAMP

Abstract

We developed a mathematical model to describe the transmission of new coronavirus in the São Paulo State, Brazil. The model divided a community in subpopulations comprised by young and elder persons, in order to take into account higher risk of fatality among elder persons with severe CoViD-19. From data collected in the São Paulo State, we estimated the transmission and additional mortality rates, from which we calculated the basic reproduction number R_0 . From estimated parameters, estimation of the deaths due to CiViD-19 was three times lower than those found in literature. Considering isolation as a control mechanism, we varied isolation rates of young and elder persons in order to assess their epidemiological impacts. The epidemiological scenarios focused mainly on evaluating the number of severe CoViD-19 cases and deaths due to this disease when isolation is introduced in a population.

Keywords: mathematical model; numerical simulations; CoViD-19; isolation; epidemiological scenarios

1 Introduction

Coronavirus disease 2019 (CoViD-19) is caused by severe acute respiratory syndrome coronavirus 2 (SARS-CoV-2), a strain of the SARS-CoV-1 (pandemic in 2002/2003), originated in Wuhan, China, in December 2019, and spread out worldwide. World Health Organization (WHO) declared CoViD-19 pandemic on 11 March, based on its own definition: “A pandemic

*Corresponding author – email: hyunyang@ime.unicamp.br; tel: + 55 19 3521-6031

is the worldwide spread of a new disease. An influenza pandemic occurs when a new influenza virus emerges and spreads around the world, and most people do not have immunity”.

Coronavirus (RNA virus) can be transmitted by droplets that escape lungs through coughing or sneezing and infects humans (direct transmission), or they are deposited in surfaces and infects humans when in contact with this contaminated surface (indirect transmission). This virus enters in susceptible persons through nose, mouth or eyes, and infects cells in the respiratory tract, being capable of releasing millions of new virus. In serious cases, immune cells overreact and attack lung cell causing acute respiratory disease syndrome and possibly death. In general, the fatality rate in elder patients (60 years or more) is much higher than the average, and under 40 years seems to be around 0.2%. Currently, there is not vaccine, neither efficient treatment, even many drugs (cloroquine, for instance) are under clinical trial. Like all RNA-based viruses, coronavirus tends to mutate faster than DNA-viruses, but lower than influenza viruses.

Many mathematical and computational models are being used to describe current new coronavirus pandemics. In mathematical model, there is a fundamental threshold (see [1]) called the basic reproduction number, which is defined as the secondary cases produced by one case introduced in a completely susceptible population, and is denoted by R_0 . When a control mechanisms is introduced, this number is reduced, and is called as the reduced reproduction number R_r . Ferguson *et al.* [4] proposed a model in order to investigate the effects of isolation of susceptible persons. They analyzed two scenarios called by them as mitigation and suppression. Roughly, mitigation reduces the basic reproduction number R_0 , but not lower than one ($1 < R_r < R_0$), while suppression reduces the basic reproduction number lower than one ($R_r < 1$). They predicted the numbers of severe cases and deaths due to CoViD-19 without control measure, and compared them with those numbers when isolations (mitigation and suppression) are introduced as control measures. Li *et al.* discussed the role of undocumented infections [5].

In this paper we formulate a mathematical model based on ordinary differential equations aiming firstly to understand the dynamics of CoViD-19 transmission, and, using the data from São Paulo State, Brazil, estimate model parameters, and, then, study potential scenarios introducing isolation as a control mechanism.

The paper is structured as follows. In Section 2, we introduce a model, which is numerically studied in Section 3. Discussions are presented in Section 4, and conclusions, in Section 5.

2 Material and methods

In a community where SARS-CoV-2 (new coronavirus) is circulating, the risk of infection is greater in elder than young persons, as well as under increased probability of being symptomatic and higher CoViD-19 induced mortality. Hence, a community is divided in two groups, comprised by young (under 60 years old, denoted by subscript y), and elder (above 60 years old, denoted by subscript o) persons. The vital dynamics of this community is given by per-capita rates of birth (ϕ) and mortality (μ).

For each sub-population j ($j = y, o$), the persons are divided in seven classes: susceptible S_j , susceptible persons who are isolated Q_j , exposed E_j , asymptomatic A_j , asymptomatic persons who are caught by test and then isolated Q_{1j} , symptomatic persons at initial phase of CoViD-19

(or pre-diseased) D_{1j} , pre-diseased persons caught by test and then isolated, plus mild CoViD-19 (or non-hospitalized) Q_{2j} , and symptomatic persons with severe CoViD-19 (hospitalized) D_{2j} . However, all persons in young and elder classes enter to same immunized class I , after experiencing infection.

With respect to new coronavirus transmission, the history of natural infection is the same in young ($j = y$) and elder ($j = o$) classes. We assume that only persons in asymptomatic (A_j) and pre-diseased (D_{1j}) classes are transmitting the virus, and other infected classes (Q_{1j} , Q_{2j} and D_{2j}) are under voluntary or forced isolation. Susceptible persons are infected according to $\lambda_j S_j/N$ and enter to classes E_j , where λ_j is the per-capita incidence rate (or force of infection) defined by $\lambda_j = \lambda(\delta_{jy} + \psi\delta_{jo})$, with λ being

$$\lambda = \beta_{1y}A_y + \beta_{2y}D_{1y} + \beta_{1o}A_o + \beta_{2o}D_{1o}, \quad (1)$$

where δ_{ij} is Kronecker delta, with $\delta_{ij} = 1$ if $i = j$, and 0, if $i \neq j$, and S_j/N is the probability of virus encountering susceptible persons. After an average period of time $1/\sigma_j$ in classes E_j , where σ_j is the incubation rate, exposed persons enter to asymptomatic A_j (with probability p_j) or pre-diseased D_{1j} (with probability $1 - p_j$) classes. After an average period of time $1/\gamma_j$ in class A_j , where γ_j is the infection rate of asymptomatic persons, symptomatic persons acquire immunity (recovered) and enter to immunized class I . Another route of exit from class A_j is being caught by a test at a rate η_j and enters to class Q_{1j} , and, then, after a period of time $1/\gamma_j$, enters to class I . With very low intensity, asymptomatic persons are in voluntary isolation, which is described by voluntary isolation rate χ_j . With respect to symptomatic persons, after an average period of time $1/\gamma_{1j}$ in class D_{1j} , where γ_{1j} is the infection rate of pre-diseased persons, pre-diseased persons enter to non-hospitalized Q_{2j} (with probability m_j) or hospitalized D_{2j} (with probability $1 - m_j$) classes. Hospitalized persons acquire immunity after a period of time $1/\gamma_{2j}$, where γ_{2j} is recovery rate of severe CoViD-19, and enter to immunized class I , or die under disease induced (additional) mortality rate α . After an average period of time $1/\gamma_j$ in class Q_{2j} , non-hospitalized persons acquire immunity and enter to immunized class I , or enter to class D_{2j} at a relapsing rate of pre-diseased persons ξ_j .

Figure 1 shows the flowchart of new coronavirus transmission model.

The new coronavirus transmission model, based on above descriptions summarized in Figure 1, is described by system of ordinary differential equations, with $j = y, o$. Equations for susceptible persons are

$$\begin{cases} \frac{d}{dt}S_y &= \phi N - (\eta_{2y} + \varphi + \mu)S_y - \lambda\frac{S_y}{N} + \eta_{3y}Q_y \\ \frac{d}{dt}S_o &= \varphi S_y - (\eta_{2o} + \mu)S_o - \lambda\psi\frac{S_o}{N} + \eta_{3o}Q_o, \end{cases} \quad (2)$$

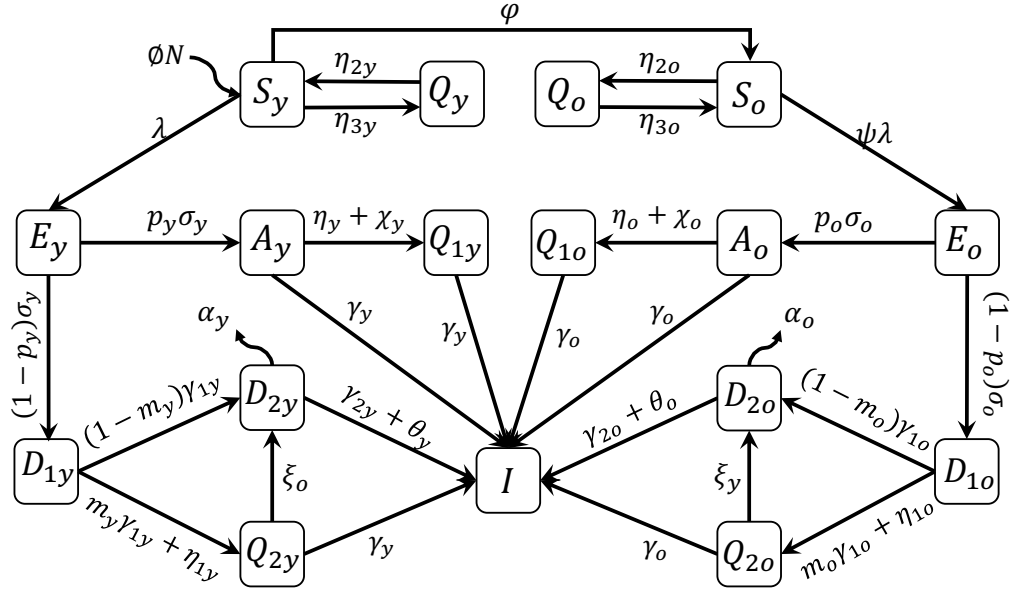


Figure 1: The flowchart of new coronavirus transmission model with variables and parameters.

for infectious persons,

$$\left\{ \begin{array}{l} \frac{d}{dt} Q_j = \eta_{2j} S_j - (\eta_{3j} + \mu) Q_j \\ \frac{d}{dt} E_j = \lambda (\delta_{jy} + \psi \delta_{jo}) \frac{S_j}{N} - (\sigma_j + \mu) E_j \\ \frac{d}{dt} A_j = p_j \sigma_j E_j - (\gamma_j + \eta_j + \chi_j + \mu) A_j \\ \frac{d}{dt} Q_{1j} = (\eta_j + \chi_j) A_j - (\gamma_j + \mu) Q_{1j} \\ \frac{d}{dt} D_{1j} = (1 - p_j) \sigma_j E_j - (\gamma_{1j} + \eta_{1j} + \mu) D_{1j} \\ \frac{d}{dt} Q_{2j} = (m_j \gamma_{1j} + \eta_{1j}) D_{1j} - (\gamma_j + \xi_j + \mu) Q_{2j}, \\ \frac{d}{dt} D_{2j} = (1 - m_j) \gamma_{1j} D_{1j} + \xi_j Q_{2j} - (\gamma_{2j} + \theta_j + \mu + \alpha_j) D_{2j}, \end{array} \right. \quad (3)$$

and for immune persons,

$$\frac{d}{dt} I = \gamma_y A_y + \gamma_y Q_{1y} + \gamma_y Q_{2y} + (\gamma_{2y} + \theta_y) D_{2y} + \gamma_o A_o + \gamma_o Q_{1o} + \gamma_o Q_{2o} + (\gamma_{2o} + \theta_o) D_{2o} - \mu I, \quad (4)$$

with $N_j = S_j + Q_j + E_j + A_j + Q_{1j} + D_{1j} + Q_{2j} + D_{2j}$ obeying, with $N = N_y + N_o + I$,

$$\frac{d}{dt} N = (\phi - \mu) N - \alpha_y D_{2y} - \alpha_o D_{2o}, \quad (5)$$

where, the initial number of population at $t = 0$ is $N(0) = N_0$. If $\phi = \mu + (\alpha_y D_{2y} + \alpha_o D_{2o}) / N$, the total size of population is constant. The initial conditions (at $t = 0$) supplied to equations (2), (3) and (4) are

$$S_j(0) = N_{0j}, \quad Q_j(0) = 0, \quad \text{and} \quad X_j(0) = n_{X_j}, \quad \text{where} \quad X_j = E_j, A_j, Q_{1j}, D_{1j}, Q_{2j}, D_{2j}, I,$$

where n_{X_j} is a non-negative number. For instance, $n_{E_y} = n_{E_o} = 0$ means that there is not any exposed persons in the beginning of epidemics.

Table 1 summarizes model variables.

Table 1: Summary of the model variables ($j = y, o$).

Symbol	Meaning
S_j	Susceptible persons
Q_j	Isolated among susceptible persons
E_j	Exposed
A_j	Asymptomatic
Q_{1j}	Isolated among asymptomatic by test
D_{1j}	Initial symptomatic (pre-diseased persons)
Q_{2j}	Isolated among pre-diseased by test
D_{2j}	Symptomatic (diseased persons)
I_j	Immune persons (recovered persons)

Table 2 summarizes model parameters and values (values for elder classes are between parentheses).

Isolation of persons deserves some words. In the modeling, the isolation is applied to susceptible persons, which are known only at exact time of the introduction of new virus, that is, $S(0) = N_0$. However, as time passes, susceptible persons are decreased and become immunized persons, and, due to asymptomatic persons, susceptible and immunized persons are indistinguishable (except caught by test and hospitalized persons). For this reason, if isolation of persons is not done at the time of virus introduction, it is probable that virus should be circulating among them, but at very lower transmission rate (virus circulates only among household and neighborhood persons).

From the system of equations (2), (3) and (4) we can derive some epidemiological parameters: new cases, new CoViD-19 cases, severe CoViD-19 cases, number of deaths due to CoViD-19, and isolated persons.

The number of persons infected with new coronavirus are given by $E_y + A_y + Q_{1y} + D_{1y} + Q_{2y} + D_{2y}$ for young persons, and $E_o + A_o + Q_{1o} + D_{1o} + Q_{2o} + D_{2o}$ for elder persons. The incidence rates are

$$\Lambda_y = \lambda \frac{S_y}{N} \quad \text{and} \quad \Lambda_o = \lambda \psi \frac{S_o}{N}, \quad (6)$$

where the per-capita incidence rate λ is given by equation (1), and the numbers of new cases C_y and C_o are

$$\frac{d}{dt} C_y = \Lambda_y dt \quad \text{and} \quad \frac{d}{dt} C_o = \Lambda_o dt,$$

Table 2: Summary of the model parameters ($j = y, o$) and values (rates in $days^{-1}$, time in $days$ and proportions are dimensionless). Some values are calculated (&), or varied (#), or assumed (*), or estimated (**), or not available (***)).

Symbol	Meaning	Value
μ	Natural mortality rate	$1/(75 \times 360)[6]$
ϕ	Birth rate	$1/(75 \times 360)^*$
φ	Aging rate	6.7×10^{-6}
$\sigma_y (\sigma_o)$	Incubation rate	$1/6 (1/5)[9]$
$\gamma_y (\gamma_o)$	Infection rate of asymptomatic persons	$1/10 (1/12)[9]$
$\gamma_{1y} (\gamma_{1o})$	Infection rate of pre-diseased persons	$1/3 (1/2)[9]$
$\gamma_{2y} (\gamma_{2o})$	Recovery rate of severe CoViD-19	$1/10 (1/14)[9]$
$\xi_y (\xi_{yo})$	Relapsing rate of pre-diseased persons	$0.005 (0.01)^*$
$\alpha_y (\alpha_o)$	Additional mortality rate	$0.0009 (0.009)^{**}$
$\eta_y (\eta_o)$	Testing rate among asymptomatic persons	$0 (0)^{***}$
$\chi_y (\chi_o)$	Voluntary isolation rate of asymptomatic persons	$0 (0)^*$
$\eta_{1y} (\eta_{1o})$	Testing rate among pre-diseased persons	$0 (0)^{***}$
$\eta_{2y} (\eta_{2o})$	Isolation rate of susceptible persons	$0.035 (0.035)^{\#}$
$\eta_{3y} (\eta_{3o})$	Releasing rate of isolated persons	$0.035 (0.035)^{\#}$
$\theta_y (\theta_o)$	Treatment rate	$0(0)^{***}$
$\beta_{1y} (\beta_{1o})$	Transmission rate due to asymptomatic persons	$0.77 (0.77)^{**}$
$\beta_{2y} (\beta_{2o})$	Transmission rate due to rpe-diseased persons	$0.77 (0.77)^{**}$
ψ	Scaling factor of transmission among elder persons	$1.17^{\&}$
$p_y (p_o)$	Proportion of asymptomatic persons	$0.8(0.75)^*$
$m_y (m_o)$	Proportion of mild (non-hospitalized) CoViD-19	$0.8 (0.75)[2]$

with $C_y(0) = 0$ and $C_o(0) = 0$, and the numbers of new cases in a day is

$$C_y^i = \int_{T_i}^{T_{i+1}} \Lambda_y dt = C_y(T_{i+1}) - C_y(T_i) \quad \text{and} \quad C_o^i = \int_{T_i}^{T_{i+1}} \Lambda_o dt = C_o(T_{i+1}) - C_o(T_i),$$

where $T_i = i\tau$, $\tau = T_{i+1} - T_i = 1 \text{ day}$, for $i = 1, \dots$, with $T_0 = 0$. Notice that C_y^i and C_o^i are entering in exposed classes at each day.

The numbers of CoViD-19 cases Δ_y and Δ_o are given by outflux of A_y , D_{1y} , A_o and D_{1o} , that is,

$$\frac{d}{dt} \Delta_y = \eta_y A_y + (\gamma_{1y} + \eta_{1y}) D_{1y} \quad \text{and} \quad \frac{d}{dt} \Delta_o = \eta_o A_o + (\gamma_{1o} + \eta_{1o}) D_{1o},$$

with $\Delta_y(0) = 0$ and $\Delta_o(0) = 0$, and the numbers of CoViD-19 cases in a day are

$$\left\{ \begin{array}{l} \Delta_y^i = \int_{T_i}^{T_{i+1}} [\eta_y A_y + (\gamma_{1y} + \eta_{1y}) D_{1y}] dt = \Delta_y(T_{i+1}) - \Delta_y(T_i) \\ \Delta_o^i = \int_{T_i}^{T_{i+1}} [\eta_o A_o + (\gamma_{1o} + \eta_{1o}) D_{1o}] dy = \Delta_o(T_{i+1}) - \Delta_o(T_i), \end{array} \right.$$

which are entering in classes Q_{1y} , D_{2y} , Q_{2y} , Q_{1o} , D_{2o} and Q_{2o} at each day.

The numbers of severe CoViD-19 (hospitalized) cases Ω_y and Ω_o are given by outflux of D_{1y} , Q_{2o} , D_{2o} and Q_{2y} , that is,

$$\frac{d}{dt}\Omega_y = (1 - m_y)\gamma_{1y}D_{1y} + \xi_y Q_{2y} \quad \text{and} \quad \frac{d}{dt}\Omega_o = (1 - m_o)\gamma_{1o}D_{1o} + \xi_o Q_{2o}, \quad (7)$$

with $\Omega_y(0) = 0$ and $\Omega_o(0) = 0$, and the numbers of hospitalized cases in a day are

$$\begin{cases} \Omega_y^i = \int_{T_i}^{T_{i+1}} [(1 - m_y)\gamma_{1y}D_{1y} + \xi_y Q_{2y}] dt = \Omega_y(T_{i+1}) - \Omega_y(T_i) \\ \Omega_o^i = \int_{T_i}^{T_{i+1}} [(1 - m_o)\gamma_{1o}D_{1o} + \xi_o Q_{2o}] dt = \Omega_o(T_{i+1}) - \Omega_o(T_i), \end{cases}$$

which are entering in classes D_{2y} and D_{2o} at each day.

The number of deaths caused by severe CoViD-19 cases Π can be calculated from hospitalized cases. This number of deaths is

$$\frac{d}{dt}\Pi = \alpha_y D_{2y} + \alpha_o D_{2o}, \quad (8)$$

with $\Pi(0) = 0$. The number of died persons in a day is

$$\pi = \pi_y + \pi_o \quad \text{with} \quad \begin{cases} \pi_y = \int_{T_i}^{T_{i+1}} \alpha_y D_{2y} dt \\ \pi_o = \int_{T_i}^{T_{i+1}} \alpha_o D_{2o} dt, \end{cases}$$

where π_y and π_o are the numbers of deaths of young and elder persons at each day.

The number of susceptible persons in isolation in the absence of releasing is obtained from

$$S^{is} = S_y^{is} + S_o^{is}, \quad \text{where} \quad \begin{cases} \frac{d}{dt}S_y^{is} = \eta_{2y}S_y, \quad \text{with} \quad S_y^{is}(0) = 0 \\ \frac{d}{dt}S_o^{is} = \eta_{2o}S_o, \quad \text{with} \quad S_o^{is}(0) = 0, \end{cases} \quad (9)$$

where the corresponding fractions of isolated susceptible persons are $f_y^{is} = S_y^{is}/N_y$ and $f_o^{is} = S_o^{is}/N_o$.

The system of equations (2), (3) and (4) is non-autonomous. Nevertheless the fractions of persons in each compartment approach to the steady state (see Appendix A), hence, by using equations (A.8) and (A.9), the reduced reproduction number R_r is given by

$$R_r = R_{ry} + R_{ro} = [p_y R_{0y}^1 + (1 - p_y) R_{0y}^2] \frac{S_y^0}{N_0} + [p_o R_{0o}^1 + (1 - p_o) R_{0o}^2] \frac{S_o^0}{N_0}, \quad (10)$$

where s_y^0 and s_o^0 are substituted by S_y^0/N_0 and S_o^0/N_0 .

Given N and R_0 , let us evaluate the number of susceptible persons in order to trigger and maintain epidemics, but in a special case. Assume that all model parameters for young

and elder classes and all transmission rates are equal, then $R_0 = \sigma\beta / [(\sigma + \phi)(\gamma + \phi)]$ and $R_e = R_0 S/N$, using approximated R_e given by equation (A.11). Letting $R_e = 1$, the critical number of susceptible persons S^{th} at equilibrium is

$$S^{th} \approx \frac{N}{R_0}. \quad (11)$$

If $S > S^{th}$, epidemics occurs and persists ($R_e > 1$, non-trivial equilibrium point P^*), and the fraction of susceptible individuals is $s^* = 1/R_e$, where $s^* = s_y^* + s_o^*$; but if $S < S^{th}$, epidemics occurs but fades out ($R_e < 1$, trivial equilibrium point P^0), and the fractions of susceptible individuals s_y and s_o at equilibrium are given by equation (A.4), or (A.12) if there is not any control.

Let us now evaluate the critical isolation rate of susceptible persons η_2 assuming that all model parameters for young and elder classes and all transmission rates are equal. In this special case, $R_r = R_0(\eta_3 + \phi) / (\eta_2 + \eta_3 + \phi)$, where $R_0 = \sigma\beta / [(\sigma + \phi)(\gamma + \phi)]$, and letting $R_r = 1$, we obtain

$$\eta_2^{th} \approx (\eta_3 + \phi)(R_0 - 1). \quad (12)$$

If $\eta_2 < \eta_2^{th}$, epidemics occurs and persists ($R_e > 1$, non-trivial equilibrium point P^*); but if $\eta_2 > \eta_2^{th}$, epidemics occurs but fades out ($R_e < 1$, trivial equilibrium point P^0).

We apply above results to study the introduction and establishment of new coronavirus in the São Paulo State, Brazil. From data collected in the São Paulo State from March 14, 2020 until April 5, 2020, we estimate transmission and additional mortality rates, and, then, study potential scenarios introducing isolation as control mechanisms.

3 Results

Results obtained in foregoing section is applied to describe new coronavirus infection in the São Paulo State, Brazil. The first confirmed case of CoViD-19, occurred in February 26, 2020, was from a traveler returning from Italy in February 21, and being hospitalized in February 24. The first death due to CoViD-19 was a 62 years old male with comorbidity who never travelled to abroad, hence considered as autochthonous transmission. He manifested first symptoms in March 10, was hospitalized in March 14, and died in March 16. In March 24, the São Paulo State authorities ordered isolation of persons acting in non-essential activities, as well as students of all level until April 6, further the isolation was extended to April 22.

Let us determine the initial conditions. In the São Paulo State, the number of inhabitants is $N(0) = N_0 = 44.6 \times 10^6$ according to SEADE [6]. The value of parameter φ given in Table 1 was calculated by equation (A.12), $\varphi = b\phi / (1 - b)$, where b is the proportion of elder persons. Using $b = 0.153$ in the São Paulo State [6], we obtained $\varphi = 6.7 \times 10^{-6} \text{ days}^{-1}$, hence, $N_y(0) = N_{0y} = 37.8 \times 10^6$ ($\bar{s}_y^0 = N_{0y}/N_y(0) = 0.8475$) and $N_o(0) = N_{0o} = 6.8 \times 10^6$ ($\bar{s}_o^0 = N_{0o}/N_o(0) = 0.1525$). The initial conditions for susceptible persons are let to be $S_y(0) = N_y(0)$ and $S_o(0) = N_o(0)$. For other variables, from Table 2, $p_y = 0.8$ and $m_y = 0.8$, the ratio asymptomatic:symptomatic is 4 : 1, and the ratio mild:severe (non-hospitalized:hospitalized) CoViD-19 is 4 : 1. We use these ratios for elder persons, even p_o and m_o are slightly different. Hence, if we assume that there is 1 person in D_{2j} (the first confirmed case), then there are 4

persons in Q_{2j} . The sum (5) is the number of persons in class D_{1j} , implying that there are 20 in class A_j , hence, the sum (25) is the number of persons in class E_j . Finally, we suppose that no one is isolated or tested, and also immunized. (Probably the first confirmed COViD-19 person transmitted the virus (since February 21 when returned infected from Italy), as well as other asymptomatic travelers returning from abroad.)

Therefore, the initial conditions supplied to the dynamic system (2), (3) and (4) are

$$\begin{cases} S_j(0) = N_{0j}, & Q_j(0) = Q_{1j}(0) = 0, & E_j(0) = 25, \\ A_j(0) = 20, & D_{1j}(0) = 5, & Q_{2j}(0) = 4 & D_{2j}(0) = 1, & I(0) = 0, \end{cases}$$

where the initial simulation time $t = 0$ corresponds to calendar time February 26, 2020, when the first case was confirmed. The system of equations (2), (3) and (4) is evaluated numerically using 4th order Runge-Kutta method.

This section presents parameters estimation and epidemiological scenarios considering isolation as control measure. In estimation and epidemiological scenarios, we assume that all transmission rates in young persons are equal, as well as in elder persons, that is, we assume that

$$\beta_y = \beta_{1y} = \beta_{2y} = \beta_{1o} = \beta_{2o}, \quad \text{and} \quad \beta_o = \psi\beta_y,$$

hence the forces of infection are $\lambda_y = (A_y + D_{1y} + A_o + D_{1o})\beta_y$ and $\lambda_o = \psi\lambda_y$.

3.1 Parameters estimation

Reliable estimation of both transmission and additional mortality rates are crucial aiming the prediction of new cases (to adequate the number of beds in hospital, for instance) and deaths. When the estimation is based on few number of data, that is, in the beginning of epidemics, some cautions must be taken, because the rates maybe over or under estimated. The reason is that in the very beginning phase of epidemics, the spreading out of infection and deaths increase exponentially without bound.

Currently, there is not sufficient number of kits to detect infection by new coronavirus. For this reason, tests to confirm infection by this virus is done only in hospitalized persons, and, also, in persons who died manifesting symptoms of CoViD-19. Hence, we have only data of hospitalized persons (D_{2y} and D_{2o}) and those who died (Π_y and Π_o). Taking into account hospitalized persons with CoViD-19, we estimate the transmission rates, and from persons died due to CoViD-19, we estimate the additional mortality rates. These rates are estimated applying the least square method (see [14]).

The introduction of quarantine is $t = 27$, corresponding to calendar time March 24, but the effects are expected to appear later. Hence, we will estimate taking into account confirmed cases and deaths from February 26 ($t = 0$) to April 5 ($t = 39$),¹ hence $n = 40$ observations. Notice that the sum of incubation and recovery periods (see Table 2) is around 16 days, hence it is expected that at around simulation time $t = 43$ (April 10) the effects of isolation appear.

To estimate the transmission rates β_y and β_o , we let $\alpha_y = \alpha_o = 0$ and the system of equations

¹Simulations were done in April 6.

(2), (3) and (4) is evaluated and calculate

$$\min \sum_{i=1}^n \{ \Omega_y(t_i) + \Omega_o(t_i) - [D_{2y}^{ob}(t_i) + D_{2o}^{ob}(t_i)] \}^2, \quad (13)$$

where min stands for minimum value, n is the number of observations, t_i is i -th observation time, Ω_y and Ω_o are given by equation (7), and D_{2y}^{ob} and D_{2o}^{ob} are observed number of hospitalized persons. The better transmission rates are those minimizing the square difference

To estimate the mortality rates α_y and α_o , we fix previously transmission rates β_y and β_o and the system of equations (2), (3) and (4) is evaluated and calculate

$$\min \sum_{i=1}^n \{ \Pi_y(t_i) + \Pi_o(t_i) - [P_y^{ob}(t_i) + P_o^{ob}(t_i)] \}^2, \quad (14)$$

where min stands for minimum value, n is the number of observations, t_i is i -th observation time, Π_y and Π_o are given by equation (8), and P_y^{ob} and P_o^{ob} are observed number of died persons. The better mortality rates are those minimizing the square difference.

Instead of using equations (13) and (14), the least square estimation method, we vary transmission or additional mortality rates and choose better fittings by evaluating the sum of squared distances between curve and data.

3.1.1 Estimation of transmission and additional mortality rates

Firstly, letting additional mortality rates equal to zero ($\alpha_y = \alpha_o = 0$), we estimate a unique $\beta = \beta_y = \beta_o$, with $\psi = 1$, against hospitalized CoViD-19 cases (D_2) data from the São Paulo State. The estimated value is $\beta = 0.8 \text{ days}^{-1}$, resulting, for the basic reproduction number, $R_0 = 6.99$ (partials $R_{0y} = 5.83$ and $R_{0o} = 1.16$). Around this value, we vary β_y and β_o and choose better fitted values comparing curves of $D_2 = D_{2y} + D_{2o}$ with observed data. The estimated values are $\beta_y = 0.77$ and $\beta_o = \psi\beta_y = 0.9009 \text{ (days}^{-1}\text{)}$, where $\Psi = 1.17$, resulting in the basic reproduction number $R_0 = 6.915$ (partials $R_{0y} = 5.606$ and $R_{0o} = 1.309$). Figure 2 shows the estimated curve of D_2 and observed data. This estimated curve is quite the same as the curve fitted using a unique β .

Fixing previously estimated transmission rates $\beta_y = 0.77$ and $\beta_o = 0.9009$ (both days^{-1}), we estimate additional mortality rates α_y and α_o . We vary α_y and α_o and choose better fitted values comparing curves of deaths due to CoViD-19 $\Pi = \Pi_y + \Pi_o$ with observed data. By the fact that lethality among young persons is much lower than elder persons, we let $\alpha_y = 0.1\alpha_o$ [9], and fit only one variable α_o . The estimated rates are $\alpha_y = 0.0036$ and $\alpha_o = 0.036 \text{ (days}^{-1}\text{)}$. Figure 3 shows the estimated curve of $\Pi = \Pi_y + \Pi_o$ and observed data. We call this as the first estimation method

The first estimation method used only one information: the risk of death is higher among elder than young persons (we used $\alpha_y = 0.1\alpha_o$). However, the lethality among hospitalized elder persons is 10% [2]. Combining both findings, we assume that the numbers of deaths for young and elder persons are, respectively, 10% and 1% of accumulated cases when Ω_y and Ω_o approach plateaus (see Figure 6 below). This is called as second estimation method, which takes into account a second information besides the one used in the first estimation method. In

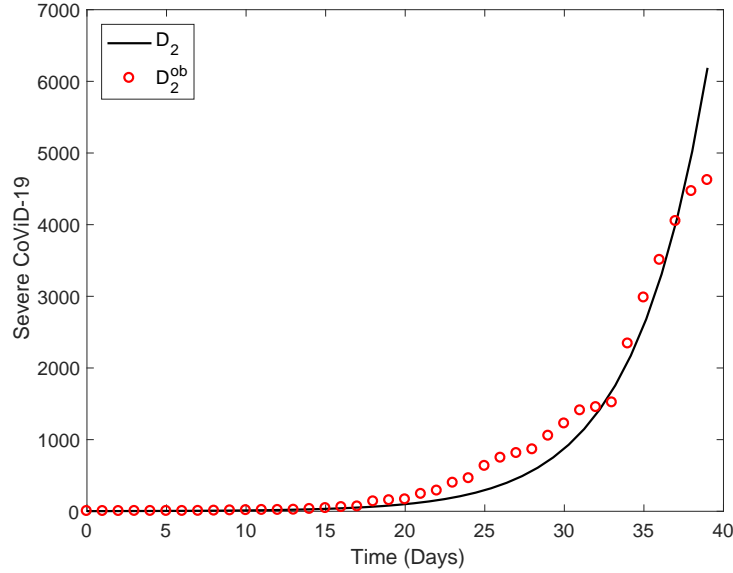


Figure 2: The estimated curve of severe CoViD-19 cases D_2 and observed data. Estimation of transmission parameters $\beta_y = 0.77$ and $\beta_o = 0.9009$ ($days^{-1}$).

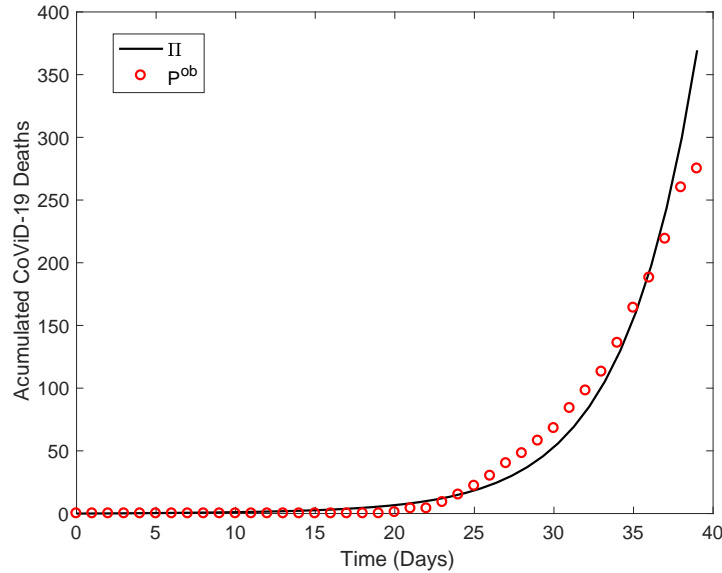


Figure 3: The estimated curve of deaths due to CoViD-19 Π and observed data. First estimation method for additional mortality rates $\alpha_y = 0.0036$ and $\alpha_o = 0.036$ ($days^{-1}$).

this procedure, the estimated rates are $\alpha_y = 0.0009$ and $\alpha_o = 0.009$ ($days^{-1}$). Figure 4 shows this estimated curve $\Pi = \Pi_y + \Pi_o$ and observe data, which fits very badly in the initial phase of epidemics, but portrays current epidemiological findings.

The fitted β_y , β_o , α_y and α_o (two estimation methods) are fixed, and control variables η_{2y}

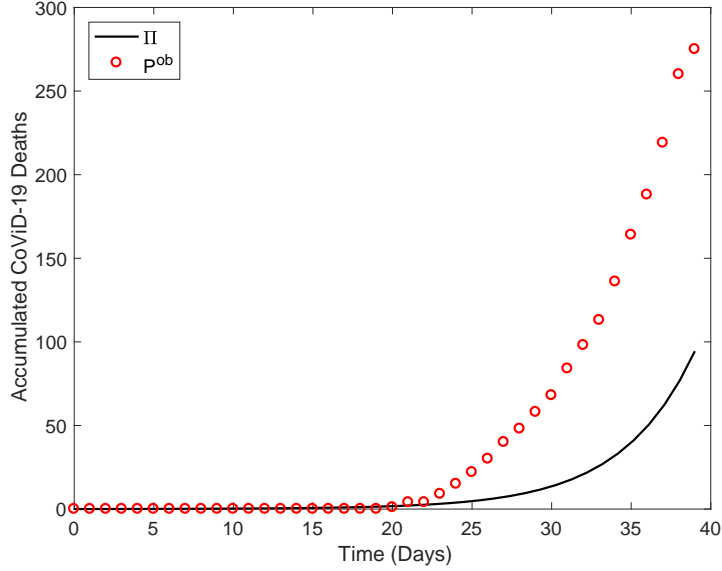


Figure 4: The estimated curve of deaths due to CoViD-19 Π and observe data. Second estimation method for additional mortality rates $\alpha_y = 0.0009$ and $\alpha_o = 0.009$ ($days^{-1}$).

and η_{2o} are varied aiming to obtain of epidemiological scenarios. In general, the epidemic period of infection by viruses τ is around 2 years, and depending on the value of R_0 , a second epidemics occurs after elapsed many years [10]. For this reason, we analyze epidemiological scenarios of CoViD-19 restricted during the first wave of epidemics letting $\tau = 140$ days.

Remembering that human population is varying due to the additional mortality (fatality) of severe CoViD-19, we have, at $t = 0$, $N_{0y} = 3.780 \times 10^7$, $N_{0o} = 0.680 \times 10^7$ and $N_0 = N_{0y} + N_{0o} = 4.460 \times 10^7$, and at $t = 140$ days, $N_y = 3.773 \times 10^7$ (0.185%), $N_o = 0.662 \times 10^7$ (2,647%) and $N = 4.435 \times 10^7$ (0.56%) for the first estimation method, and $N_y = 3.778 \times 10^7$ (0.052%), $N_o = 0.674 \times 10^7$ (0.882%) and $N = 4.452 \times 10^7$ (0.179%) for the second estimation method. The percentage of deaths ($100(N_{0j} - N_j)/N_{0j}$) is given between parentheses. The first estimation method for α_y and α_o yielded higher number of deaths than the second method.

3.1.2 Epidemiological scenario without any control mechanisms

All effects of isolation will be compared with new coronavirus transmission without any control. Initially, estimated curves will be extended until $\tau = 140$ days, when disease attains low values.

Figure 5 shows the estimated curves of the number of hospitalized (severe) CoViD-19 (D_{2y} , D_{2o} and $D_2 = D_{2y} + D_{2o}$). We observe that the peaks of severe CoViD-19 are for elder, young and all persons are, respectively, 2.061×10^5 , 5.532×10^5 and 7.582×10^5 , which occur at same time $t = 72$ days.

Figure 6 shows the estimated curves of accumulated number of severe CoViD-19 (Ω_y , Ω_o and $\Omega = \Omega_y + \Omega_o$), from equation (7). At $t = 140$ days, Ω is approaching to asymptote (or plateau), which can be understood as the time when the first wave of epidemics ends. The curves Ω_y , Ω_o and Ω attain values at $t = 140$, respectively, 1.798×10^6 , 0.563×10^6 and 2.361×10^6 .

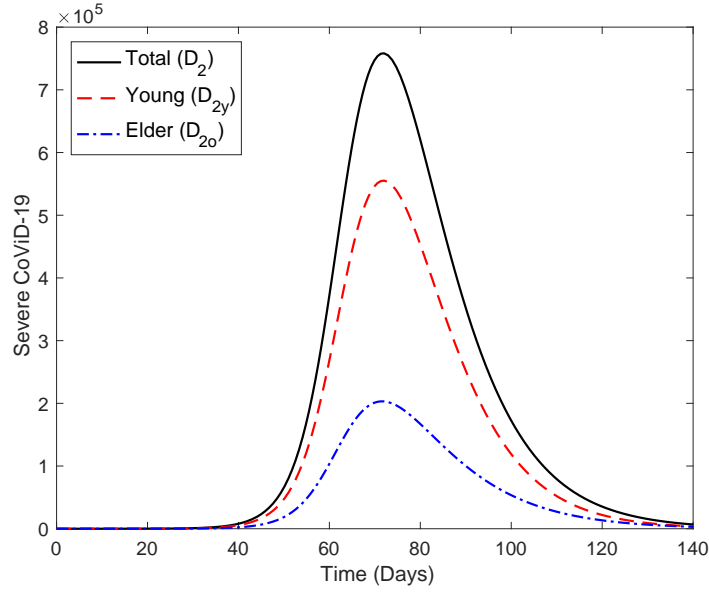


Figure 5: The estimated curves of the number of hospitalized (severe) CoViD-19 (D_{2y} , D_{2o} and $D_2 = D_{2y} + D_{2o}$) during the first wave of epidemics.

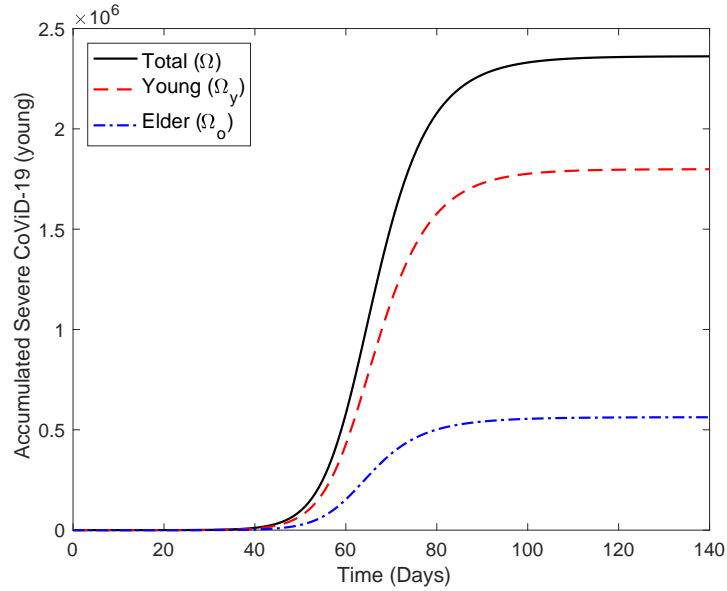


Figure 6: The estimated curves of accumulated number of severe CoViD-19 (Ω_y , Ω_o and $\Omega = \Omega_y + \Omega_o$) during the first wave of epidemics.

Figure 7 shows the estimated curves of accumulated number of CoViD-19 deaths (Π_y , Π_o and $\Pi = \Pi_y + \Pi_o$), from equation (8). At $t = 140$ days, Π is approaching to plateau. The values of Π_y , Π_o and Π are at $t = 140$, for the first method of estimation, respectively, 0.6235×10^5

(3.47%), 1.883×10^5 (33.4%) and 2.507×10^5 (10.62%), and for the second method of estimation, respectively, 1.60×10^4 (0.89%), 6.265×10^4 (11.13%) and 7.865×10^4 (3.33%). Percentage between parentheses is the ratio Π/Ω . The second estimation method is shown in Figure 7.

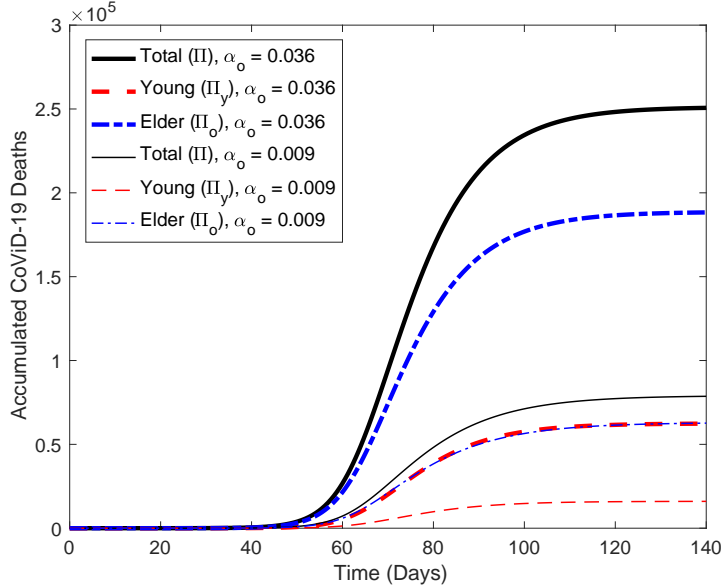


Figure 7: The estimated curves of accumulated number of CoViD-19 deaths (Π_y , Π_o and $\Pi = \Pi_y + \Pi_o$) during the first wave of epidemics.

By comparing percentages between deaths due to CoViD-19 (Π) and accumulated severe CoViD-19 cases (Ω), the first method predicts at least 3-times that predicted by the second method. Especially among elder persons, second method predicts 11.13%, three times lower than 33.4% predicted by the first method. Hence, the second estimation is more credible than the first one. Hence, we will adopt the second estimation method for additional mortality rates, $\alpha_y = 0.0009$ and $\alpha_o = 0.009$ ($days^{-1}$) hereafter except explicitly cited. Remember that additional mortality rates are considered constant in all time.

Figure 8 shows the curves of the number of susceptible persons (S_y , S_o and $S = S_y + S_o$). At $t = 0$, the numbers of S_y , S_o and S are, respectively, 3.77762×10^7 , 0.68238×10^7 and 4.46×10^7 , and diminish due to infection, to lower values at $t = 140$ days. Notice that, after the first wave of epidemics, very few number of susceptible persons are left behind, which are 1.23880×10^5 (0.33%), 0.02643×10^5 (0.039%) and 1.26523×10^5 (0.28%), for young, elder and total persons, respectively. Percentage between parentheses is the ratio $S(140)/S(0)$.

Figure 9 shows the curves of the number of immune persons (I_y , I_o and $I = I_y + I_o$). At $t = 0$, the number of immune persons I_y , I_o and I increase from zero to, respectively, 3.76156×10^7 (99.57%), 0.67234×10^7 (98.53%) and 4.43390×10^7 (99.41%) at $t = 140$ days. Percentage between parentheses is the ratio $I/S(0)$.

From Figures 8 and 9, the difference between percentages of $I/S(0)$ and $S(140)/S(0)$ is the percentage of all persons who have had contact with new coronavirus. Hence, the second wave of epidemics will be triggered after elapsed very long period time waiting the accumulation of

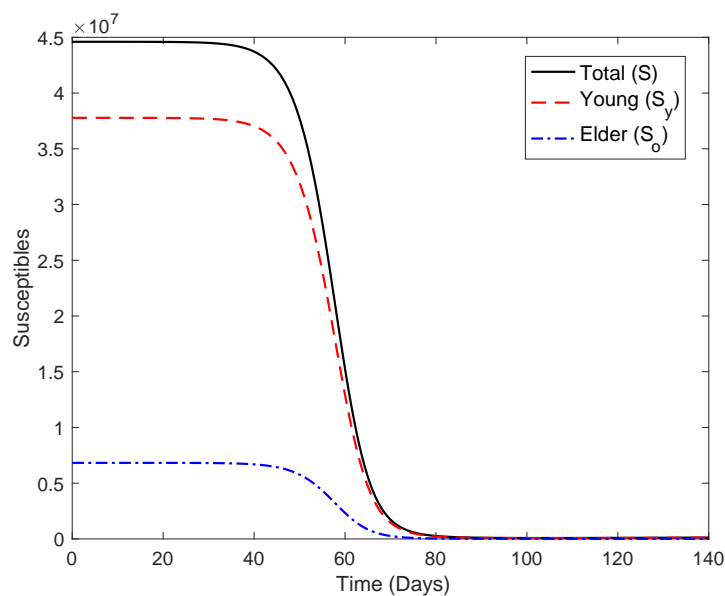


Figure 8: The curves of the number of susceptible persons (S_y , S_o and $S = S_y + S_o$) during the first wave of epidemics.

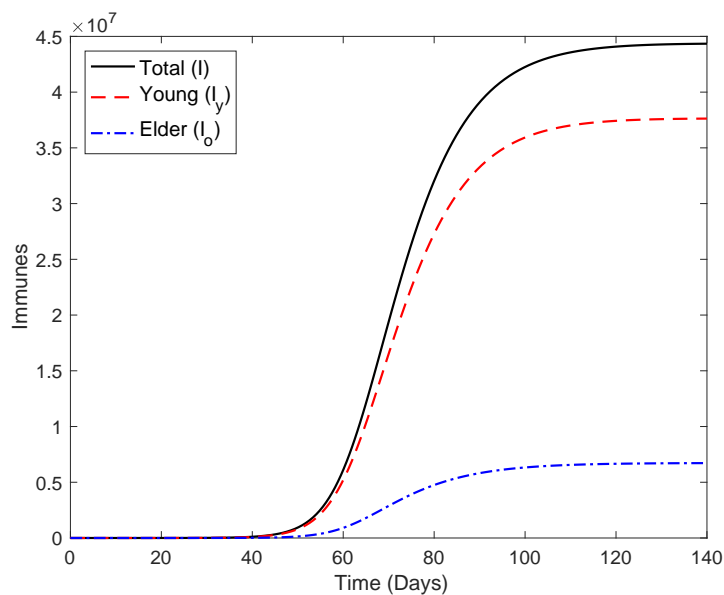


Figure 9: The curves of the number of immune persons (I_y , I_o and $I = I_y + I_o$) during the first wave of epidemics.

susceptible persons to surpass its critical number [10] [13]. Simulating the system of equations (2), (3) and (4) for a very long time (figures not shown), the trajectories reach the equilibrium values for susceptible persons ($s_y^* = S_y^*/N^* = 0.14660$, $s_o^* = S_o^*/N^* = 0.00348$ and $s^* = s_y^* + s_o^* =$

0.15008).

Let us estimate roughly the critical number of susceptible persons S^{th} from equation (11). For $R_0 = 6.915$, $S^{th} = 6.450 \times 10^6$. Hence, for the São Paulo State, isolating 38.15 million (85.5%) or above persons is necessary to avoid persistence of epidemics. The number of young persons is 3.5 million less than the threshold number of isolated persons to guarantee eradication of CoViD-19. Another rough estimation is done to isolation rate of susceptible persons η_2 , letting $\eta_3 = 0$ in equation (12), resulting in $\eta^{th} = 2.19 \times 10^{-4} \text{ years}^{-1}$, for $R_0 = 6.915$. Then, for $\eta > \eta^{th}$ the new coronavirus epidemics fades out.

3.2 Epidemiological scenarios considering control mechanisms

Using estimated transmission and additional mortality rates, we solve numerically the system of equations (2), (3) and (4) considering only one control mechanism, that is, the isolation, due to the fact that there is few number of testing kits, and treatment and vaccine are not available yet.

In this section we fix the estimated transmission rates as $\beta_y = 0.77$ and $\beta_o = \psi\beta_y = 0.9009$ (days^{-1}), and the additional mortality rates, $\alpha_y = 0.0009$ and $\alpha_o = 0.009$ (days^{-1}).

We consider two cases: Isolation without subsequent releasing of isolated persons, and isolation followed by releasing of these persons. By varying isolation parameters η_{2y} and η_{2o} , and releasing parameters η_{3y} and η_{3o} , we present some epidemiological scenarios. In all scenarios, t is simulation time, instead of calendar time.

3.2.1 Scenarios – Isolation without releasing ($\eta_{3y} = \eta_{3o} = 0$)

At $t = 0$ (February 26) the first case of severe CiViD-19 was confirmed, and at $t = 27$ (March 24) isolation as mechanism of control (described by η_{2y} and η_{2o}) was introduced until April 22. We analyze two cases. First, there is indiscriminated isolation for young and elder persons, hence we assume that the same rates of isolation are applied to young and elder persons, that is, $\eta_2 = \eta_{2y} = \eta_{2o}$. Further, there is discriminated (preferential) isolation of elder persons, hence we assume that $\eta_{2o} \neq \eta_{2y}$.

Regime 1 – Equal isolation of young and elder persons ($\eta_2 = \eta_{2y} = \eta_{2o}$) In regime 1, we call equal isolation of young and elder persons in the sense of equal isolation rates. Recalling that η_{2y} and η_{2o} are per-capita rates, both rates isolate proportionally young and elder persons, but the actual number of isolation is higher among young persons.

We choose 7 different values for the isolation rate η_2 (days^{-1}) applied to young and elder persons. The values for η_2 : 0.00021 ($R_r = 1$), 0.001 ($R_r = 0.23$), 0.005 ($R_r = 0.048$), 0.01 ($R_r = 0.024$), 0.015 ($R_r = 0.016$), 0.025 ($R_r = 0.009$) and 0.035 ($R_r = 0.007$). The value for the reduced reproduction number is R_r is calculated from equation (10). For $\eta_2 = 0.035$, the reduced reproduction number with respect to the basic reproduction number is reduced in 0.1%. In all figures, the case $\eta_2 = 0$ ($R_0 = 6.915$) is also shown.

Figure 10 shows curves of severe cases of CoViD-19 D_{2j} , $j = y, o$, without and with isolation for different values of η_2 . Notice that first two curves obtained with $\eta_2 = 0$ and 0.00021 practically coincide, and the latter is slightly lower than the roughly estimated $\eta^{th} = 2.19 \times 10^{-4}$

$years^{-1}$. We present values of peak for three values of η_2 . For $\eta_2 = 0$, the peak of young (first coordinate) and elder (second coordinate) persons are $(5.532 \times 10^5, 2.061 \times 10^5)$, and for $\eta_2 = 0.01$ $(3.566 \times 10^5, 1.361 \times 10^5)$, and 0.035 $(0.699 \times 10^5, 0.292 \times 10^5)$. The time (*days*) at which the peak occurs for young (first coordinate) and elder (second coordinate) persons are for $\eta_2 = 0$ (72,71), 0.01 (75,74) and 0.035 (77,77). For $\eta_2 = 0.01$ in comparison with $\eta_2 = 0$, the peaks are reduced in 64.4% and 66.0%, respectively, for young and elder persons. For $\eta_2 = 0.035$, the peaks are reduced in 12.6% and 14.2%.

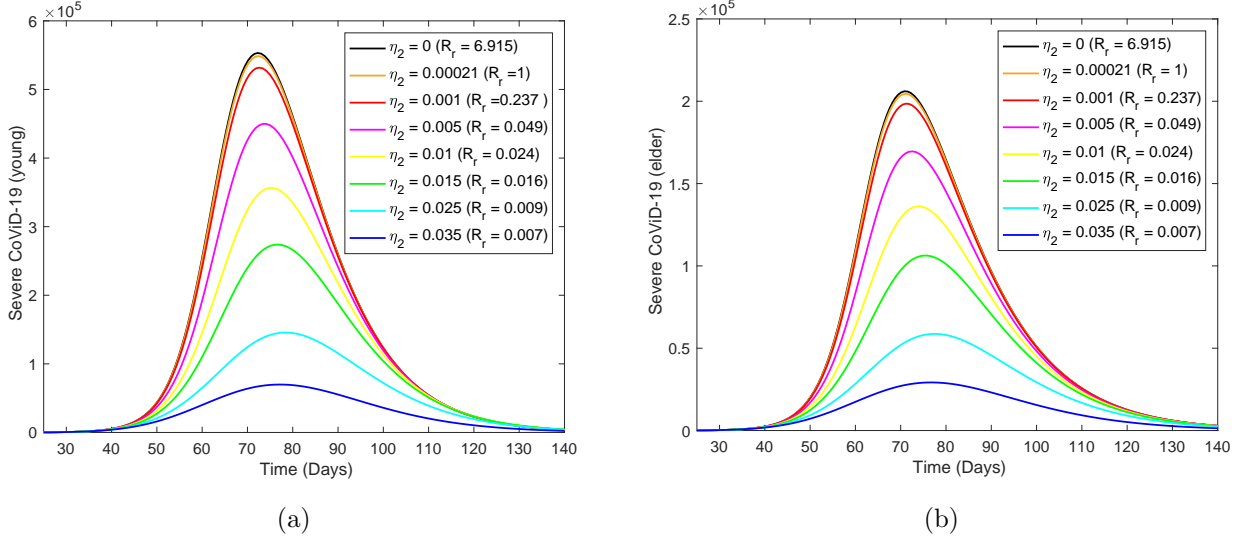


Figure 10: The curves of severe cases of CoViD-19 D_{2j} , $j = y, o$, without and with isolation for different values of η_2 . Curves from top to bottom corresponds to increasing η_2 .

As isolation parameter η_2 increases, the diminishing peaks of curves of D_{2y} and D_{2o} displace initially to right (higher times), but at $\eta_2 = \eta_2^c$, they change the direction and move leftwardly. However, all curves remain inside the curve without isolation ($\eta_2 = 0$). The values at which the peaks change direction are $\eta_{2y}^c = 0.0027 \text{ days}^{-1}$ ($t = 78.35$) and $\eta_{2o}^c = 0.0028 \text{ days}^{-1}$ ($t = 77.58$). In order to understand this phenomenon, we recall an age-structured model to describe rubella infection [11] [12]. There, as vaccination rate increases, the peaks of age-depending forces of infection initially moves to right, and, then, move leftwardly. As a consequence, the average age at the first infection increases.

At $t = 27$ isolation begun in the São Paulo State. For this reason, in the system of equations (2), (3) and (4), we let $\eta_2 = 0$ for $t < 27$, and $\eta_2 > 0$ for $t \geq 27$. In Figure 11 we show the estimated curves of severe CoViD-19 cases D_2 without ($\eta_2 = 0$ in all time) and with ($\eta_2 = 0.035 \text{ days}^{-1}$) isolation, which was introduced at $t = 27$. It seems that the effects of isolation (in observed data) appears at around $t = 38$ (April 5), 11 days after its introduction. Figure 11 shows an isolation scheme described by $\eta_2 = 0.035 \text{ days}^{-1}$ introduced at $t = 27$, which decreases the curve without isolation. The transition from without to with isolation is under very complex dynamics, for this reason we can not assure that $\eta_2 = 0.035 \text{ days}^{-1}$ is a good estimation (there are so few data). Hence, one of the curves in Figure 10 may correspond to the isolation applied in the São Paulo State.

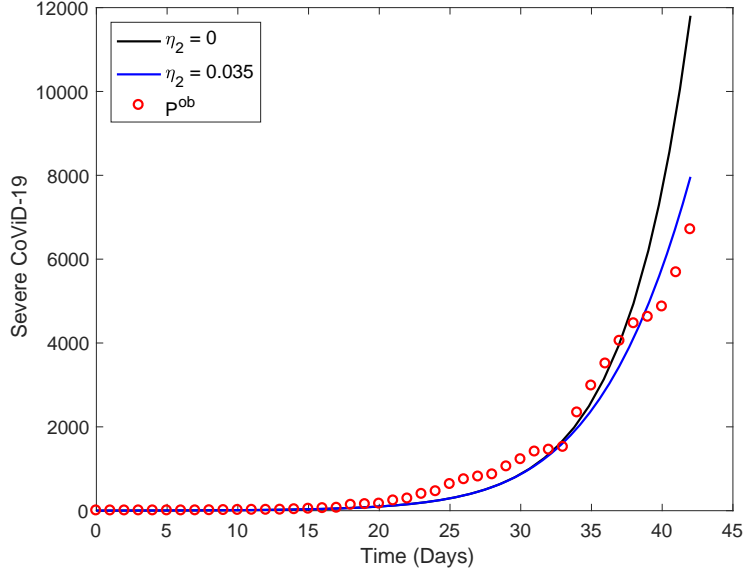


Figure 11: The curves of an isolation scheme described by $\eta_2 = 0.035 \text{ days}^{-1}$ introduced at $t = 27$, and the curve without isolation.

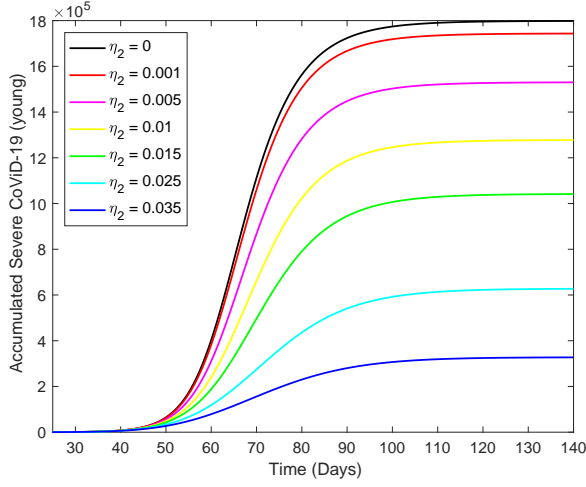
The curve corresponding to $\eta_2 = 0.00021 \text{ days}^{-1}$ in Figure 10 can be considered as a failure isolation ($R_r > 1$), for this reason this curve is removed in all following figures.

Figure 12 shows curves of accumulated cases of severe CoViD-19 Ω_j , $j = y, o$, without and with isolation for different values of η_2 . As isolation rate η_2 increases, the accumulated number of deaths due to severe CoViD-19 decreases. We present at $t = 140$ for three values of η_2 . For $\eta_2 = 0$, the number of young (first coordinate) and elder (second coordinate) persons are $(1.798 \times 10^6, 5.630 \times 10^5)$, and for $\eta_2 = 0.01$ $(1.278 \times 10^6, 4.063 \times 10^5)$, and 0.035 $(0.372 \times 10^6, 1.133 \times 10^5)$. For $\eta_2 = 0.01$ in comparison with $\eta_2 = 0$, severe CoViD-19 cases are reduced in 71.1% and 72.2%, respectively for young and elder persons. For $\eta_2 = 0.035$, severe CoViD-19 cases are reduced in 20.7% and 17.4%.

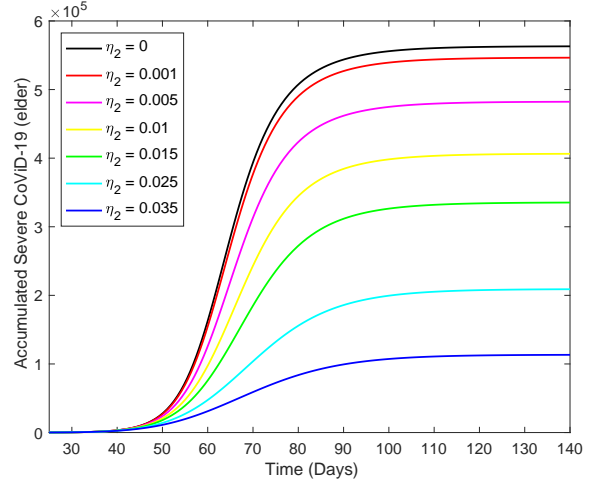
Figure 13 shows curves of accumulated cases of CoViD-19 deaths Π_j , $j = y, o$, without and with isolation for different values of η_2 . We present at $t = 140$ for three values of η_2 . For $\eta_2 = 0$, the number of young (first coordinate) and elder (second coordinate) persons are $(1.6 \times 10^4, 6.265 \times 10^4)$, and for $\eta_2 = 0.01$ $(1.135 \times 10^4, 5.514 \times 10^4)$, and 0.035 $(0.29 \times 10^4, 1.252 \times 10^4)$. For $\eta_2 = 0.01$ in comparison with $\eta_2 = 0$, death due to CoViD-19 cases are reduced in 70.9% and 88.0%, respectively for young and elder persons. For $\eta_2 = 0.035$, death due to CoViD-19 cases are reduced in 18.1% and 20.0%.

Figure 14 shows curves of the number of susceptible persons S_j , $j = y, o$, without and with isolation for different values of η_2 . We present at $t = 140$ for three values of η_2 . For $\eta_2 = 0$, the number of young (first coordinate) and elder (second coordinate) persons are $(1.239 \times 10^5, 2463)$, and for $\eta_2 = 0.01$ $(1.634 \times 10^5, 8190)$, and 0.035 $(2.492 \times 10^5, 60620)$. For $\eta_2 = 0.01$ in comparison with $\eta_2 = 0$, susceptible persons are increased in 132% and 333%, respectively for young and elder persons. For $\eta_2 = 0.035$, susceptible persons are increased in 201% and 2,461%.

As isolation parameters η_2 increases, the number of susceptible persons decreases according

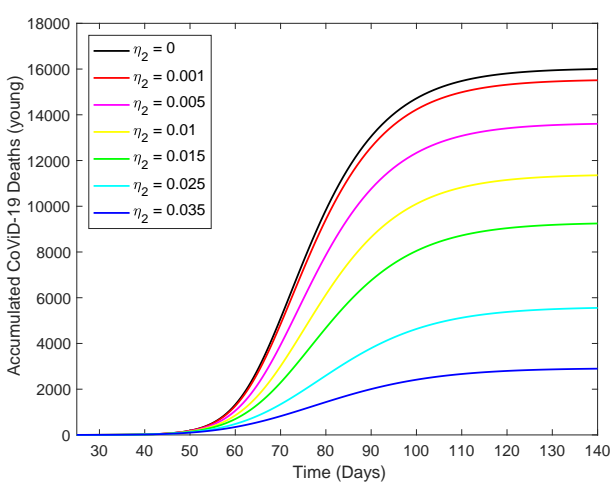


(a)

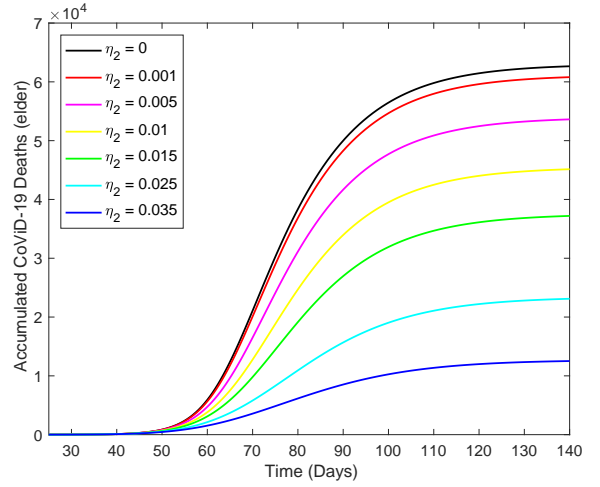


(b)

Figure 12: The curves of accumulated cases of severe CoViD-19 Ω_j , $j = y, o$, without and with isolation for different values of η_2 . Curves from top to bottom corresponds to increasing η_2 . The beginning of isolation is at $t = 27$.



(a)



(b)

Figure 13: The curves of accumulated cases of CoViD-19 deaths Π_j , $j = y, o$, without and with isolation for different values of η_2 . Curves from top to bottom corresponds to increasing η_2 . The beginning of isolation is at $t = 27$.

to sigmoid shape, but, at a sufficient higher value, follows exponential decay. Again, this phenomenon is understood recalling rubella transmission model [13]. There, as vaccination rate increases, the fraction of susceptible persons decreases following damped oscillations when $R_r > 1$, attaining non-trivial equilibrium point. However, for $R_r < 1$, there is trivial equilibrium

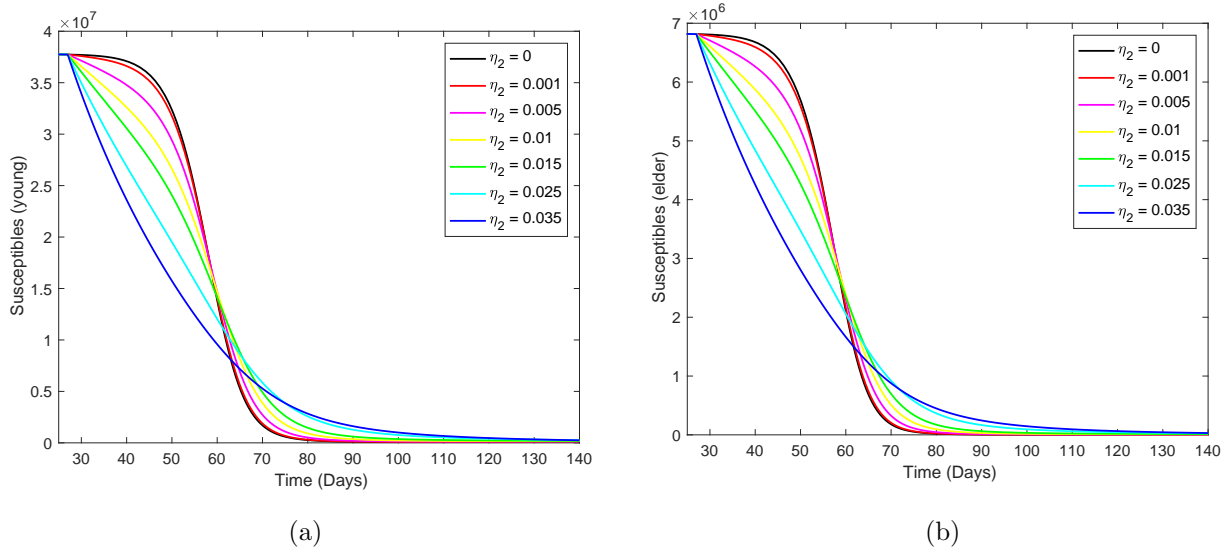


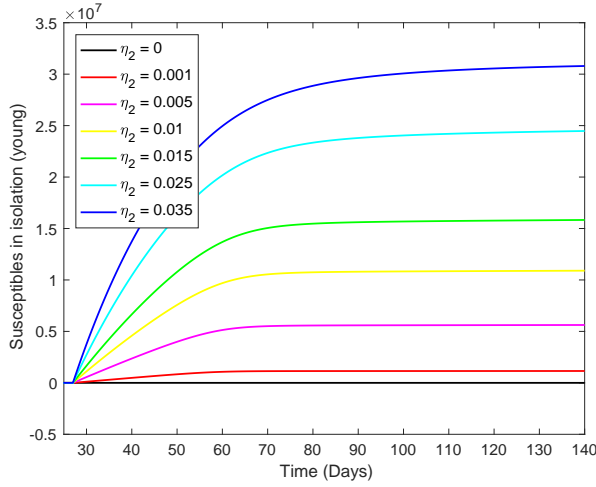
Figure 14: The curves of the number of susceptible persons S_j , $j = y, o$, without and with isolation for different values of η_2 . Curves from top to bottom corresponds to increasing η_2 . The beginning of isolation is at $t = 27$.

point and trajectories follows two pattern: (1) if R_r is not so low, the fraction of susceptible persons decreases lower than the value of trivial equilibrium point, and must increase to attain the equilibrium value, but not surpassing it (then there is not damped oscillations); and (2) if R_r is low, the fraction of susceptible persons decreases never lower than the value of trivial equilibrium point, for this reason attains this equilibrium value decaying exponentially without surpassing it in any time.

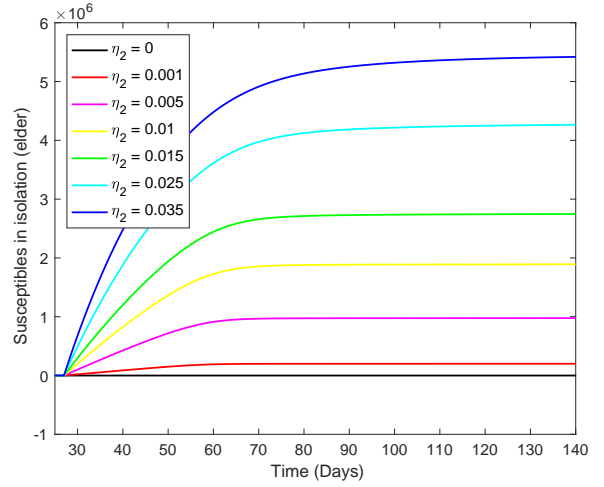
Figure 15 shows curves of the number of isolated susceptible persons S_j^{is} , $j = y, o$, with isolation for different values of η_2 , from equation (9). We present at $t = 140$ for three values of η_2 . For $\eta_2 = 0$, there is not isolated persons, and for $\eta_2 = 0.01$ ($1.09 \times 10^7, 1.892 \times 10^6$), and 0.035 ($3.079 \times 10^7, 5.419 \times 10^6$). For $\eta_2 = 0.01$ in comparison with all persons N_0 (at $t = 0$), isolated susceptible persons are 2.4% and 0.42%, respectively for young and elder persons. For $\eta_2 = 0.035$, isolated susceptible persons are 6.9% and 1.22%.

Figure 16 shows curves of the number of immune persons I_j , $j = y, o$, without and with isolation for different values of η_2 . We present at $t = 140$ for three values of η_2 . For $\eta_2 = 0$, the number of young (first coordinate) and elder (second coordinate) persons are ($3.762 \times 10^7, 6.723 \times 10^6$), and for $\eta_2 = 0.01$ ($2.671 \times 10^7, 4.849 \times 10^6$), and 0.035 ($0.683 \times 10^7, 1.349 \times 10^6$). For $\eta_2 = 0.01$ in comparison with $\eta_2 = 0$, immune persons are reduced to 71.0% and 72.1%, respectively for young and elder persons, very close to the reductions observed in deaths due to CoViD-19. For $\eta_2 = 0.035$, immune persons are reduced to 18.1% and 20.0%, very close to the reductions observed in deaths due to CoViD-19.

Immunological parameters (peak of D_2 , Ω , Π and I) are reduced quite similar for $\eta_2 = 0.035$ $days^{-1}$, between 4.8-times (21%) and 8.3-times (12%), however the susceptible persons left behind at the end of the first wave increase dramatically, 20-times (young) and 240-times

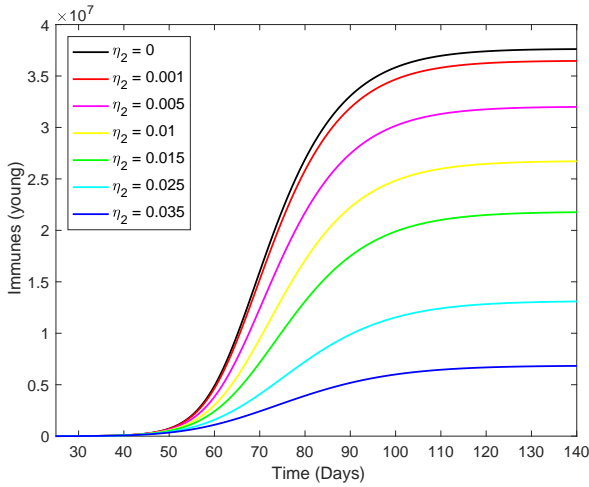


(a)

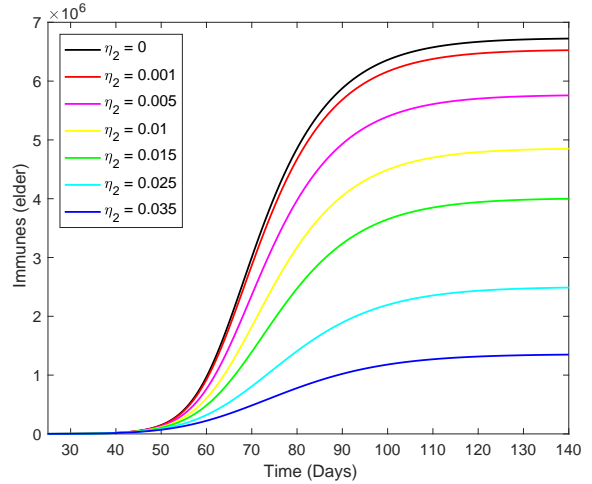


(b)

Figure 15: The curves of the number of isolated susceptible persons S_j^{is} , $j = y, o$, with isolation for different values of η_2 . Curves from top to bottom corresponds to increasing η_2 . The beginning of isolation is at $t = 27$.



(a)



(b)

Figure 16: The curves of the number of immune persons I_j , $j = y, o$, without and with isolation for different values of η_2 . Curves from top to bottom corresponds to increasing η_2 . The beginning of isolation is at $t = 27$.

(elder), with 24-times higher for elder persons. Hence, in a second wave, there will be more infections among elder persons.

Regime 2 – Different isolation of young and elder persons ($\eta_{2o} \neq \eta_{2y}$) In regime 2, we call different isolation of young and elder persons in the sense that elder isolation rate is fixed, and young isolation rate is varied, and vice-versa.

Firstly, we choose the isolation rate of elder persons $\eta_{2o} = 0.01 \text{ days}^{-1}$, and vary $\eta_{2y} = 0.001$ ($R_r = 0.235$), 0.005 ($R_r = 0.049$), 0.01 ($R_r = 0.024$), 0.015 ($R_r = 0.016$), 0.025 ($R_r = 0.009$), 0.035 ($R_r = 0.007$) and 0.1 ($R_r = 0.002$). The value for the reduced reproduction number is R_r is calculated from equation (10).

Figure 17 shows curves of severe cases of CoViD-19 D_{2j} , $j = y, o$, varying η_{2y} , fixing $\eta_{2o} = 0.01 \text{ days}^{-1}$. The decreasing pattern of D_{2y} follows that observed in regime 1, but in D_{2o} , as η_{2y} increases, the peaks displace faster to right, and the curves become more asymmetric (increased skewness) and spread beyond the curve without isolation.

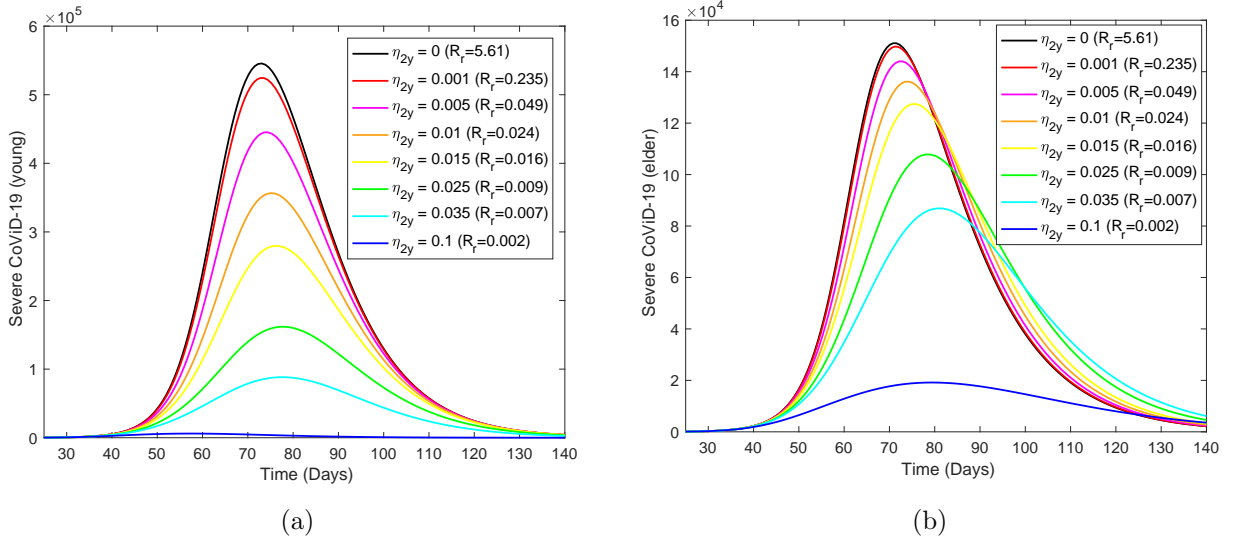


Figure 17: The curves of severe cases of CoViD-19 D_{2j} , $j = y, o$, varying η_{2y} , fixing $\eta_{2o} = 0.01 \text{ days}^{-1}$. Curves from top to bottom corresponds to increasing η_{2y} . The beginning of isolation is at $t = 27$.

Figure 18 shows curves of the number of susceptible persons S_j , $j = y, o$, varying η_{2y} , fixing $\eta_{2o} = 0.01 \text{ days}^{-1}$. The decreasing pattern of S_y follows that observed in regime 1 (sigmoid shape substituted by exponential decay), but the sigmoid shaped decreasing curves of S_o , as η_{2y} increases, move from bottom to top, which is an opposite pattern observed in regime 1. As isolation of young increases, the number of susceptible young persons decreases, but the number of susceptible elder persons increases. However, from Figure 17, severe CoViD-19 cases decrease for both subpopulations. This can be explained by the decreasing in immune persons: young immune persons decrease 41-times when η_{2y} decreases from 0.015 to 0.1, while elder persons decrease 4-times (see Table 3).

The curves of accumulated cases of severe CoViD-19 Ω , accumulated cases of CoViD-19 deaths Π , the number of isolated susceptible person S^{is} , and the number of immune persons I are similar than those shown in foregoing section. For this reason, we present in Table 3

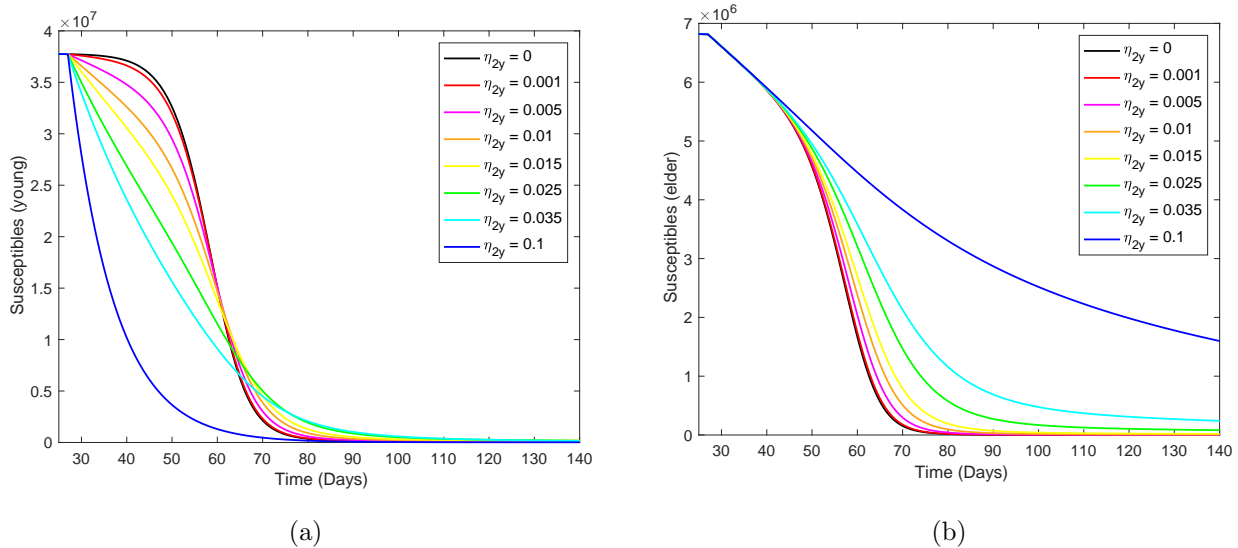


Figure 18: The curves of the number of susceptible persons S_j , $j = y, o$, varying η_{2y} , fixing $\eta_{2o} = 0.01 \text{ days}^{-1}$. Curves from top to bottom corresponds to decreasing η_{2y} . The beginning of isolation is at $t = 27$.

($\eta_{2o} = 0.01 \text{ days}^{-1}$ fixed) their values at $t = 140$ for young, elder and all persons, letting $\eta_{2y} = 0.015$, $\eta_{2y} = 0.035$ and $\eta_{2y} = 0.1 \text{ (days}^{-1}\text{)}$. For $\eta_{2o} = \eta_{2y} = 0$ we have, from foregoing section, $\Omega_y = 1.798 \times 10^6$, $\Omega_o = 5.630 \times 10^5$ and $\Omega = 2.361 \times 10^6$; $\Pi_y = 1.6 \times 10^4$, $\Pi_o = 6.265 \times 10^4$ and $\Pi = 7.865 \times 10^4$; $S_y = 1.239 \times 10^5$, $S_o = 2463$ and $S = 1.263 \times 10^5$; and $I_y = 3.762 \times 10^7$, $I_o = 6.723 \times 10^6$ and $I = 4.434 \times 10^7$. The percentages are calculated as the ratio between epidemiological parameter evaluated with ($\eta_{2j} > 0$) and without ($\eta_{2y} = \eta_{2o} = 0$) isolation, at $t = 140$. The number of isolated susceptible persons is $S^{is} = 0$ when there is not isolation, hence the percentage is the ratio between S^{is} at $t = 140$ and N_0 .

Figures 17 and 18 and Table 3 portrait preferential isolation of young persons, but maintaining elder persons isolated at a fixed level. Hence, the increasing in η_{2y} of course protects young persons, but elder persons are also benefitted .

Now, we choose the isolation rate of young persons $\eta_{2y} = 0.01 \text{ days}^{-1}$, and vary the isolation rate of elder persons $\eta_{2o} \text{ (days}^{-1}\text{)}$ for 7 different values: $\eta_{2o} = 0.001$ ($R_r = 0.025$), 0.005 ($R_r = 0.02444$), 0.01 ($R_r = 0.02442$), 0.015 ($R_r = 0.024416$), 0.025 ($R_r = 0.024413$), 0.035 ($R_r = 0.024411$) and 0.1 ($R_r = 0.02440$).

Figure 19 shows curves of severe cases of CoViD-19 D_{2j} , $j = y, o$, varying η_{2o} , fixing $\eta_{2y} = 0.01 \text{ days}^{-1}$. The same pattern observed in Figure 17, changing D_{2y} by D_{2o} , but more smooth.

Figure 20 shows curves of the number of susceptible persons S_j , $j = y, o$, varying η_{2o} , fixing $\eta_{2y} = 0.01 \text{ days}^{-1}$. The same pattern observed in Figure 18, changing S_y by S_o .

The curves of accumulated cases of severe CoViD-19 Ω , accumulated cases of CoViD-19 deaths Π , the number of isolated susceptible person S^{is} , and the number of immune persons I are similar than those shown in foregoing section. For this reason, we present in Table 4 ($\eta_{2y} = 0.01 \text{ days}^{-1}$ fixed) their values at $t = 140$ for young, elder and all persons, letting

Table 3: Values and percentages of Ω , Π , Q and I fixing $\eta_{2o} = 0.01 \text{ days}^{-1}$ and varying $\eta_{2y} = 0.015$, $\eta_{2y} = 0.035$ and $\eta_{2y} = 0.1 \text{ (days}^{-1})$. y , o and Σ stand for, respectively, young, elder and total persons.

	$\eta_{2y} = 0.015$			$\eta_{2y} = 0.035$			$\eta_{2y} = 0.1$		
	y	o	Σ	y	o	Σ	y	o	Σ
$\Omega \text{ (} 10^6 \text{)}$	1.051	0.3982	1.4492	0.396	0.3342	0.7302	0.026	0.098	0.124
Π	9330	44170	53500	3500	36700	40200	230	10540	10770
$S \text{ (} 10^5 \text{)}$	1.748	0.1907	1.9387	1.476	2.4	3.876	0.167	15.98	16.15
$Q \text{ (} 10^7 \text{)}$	1.566	0.1978	1.7638	2.945	0.252	3.197	3.739	0.4013	4.14
$I \text{ (} 10^7 \text{)}$	2.196	0.4749	2.6709	0.827	0.3966	1.224	0.054	0.1148	0.1688
$\Omega \text{ (\%)}$	58.45	70.73	61.38	22	59.36	30.93	1.45	17.41	5.25
$\Pi \text{ (\%)}$	58.31	70.50	68.02	21.88	58.58	51.11	1.44	16.82	13.69
$S \text{ (\%)}$	141.08	774.26	153.43	119.13	9744	306.74	13.48	64880	1278
$Q \text{ (\%)}$	41.45	29.00	39.55	77.95	36.95	71.68	98.97	58.84	92.82
$I \text{ (\%)}$	58.37	7.06	60.23	21.98	5.899	27.60	1.44	1.708	3.81

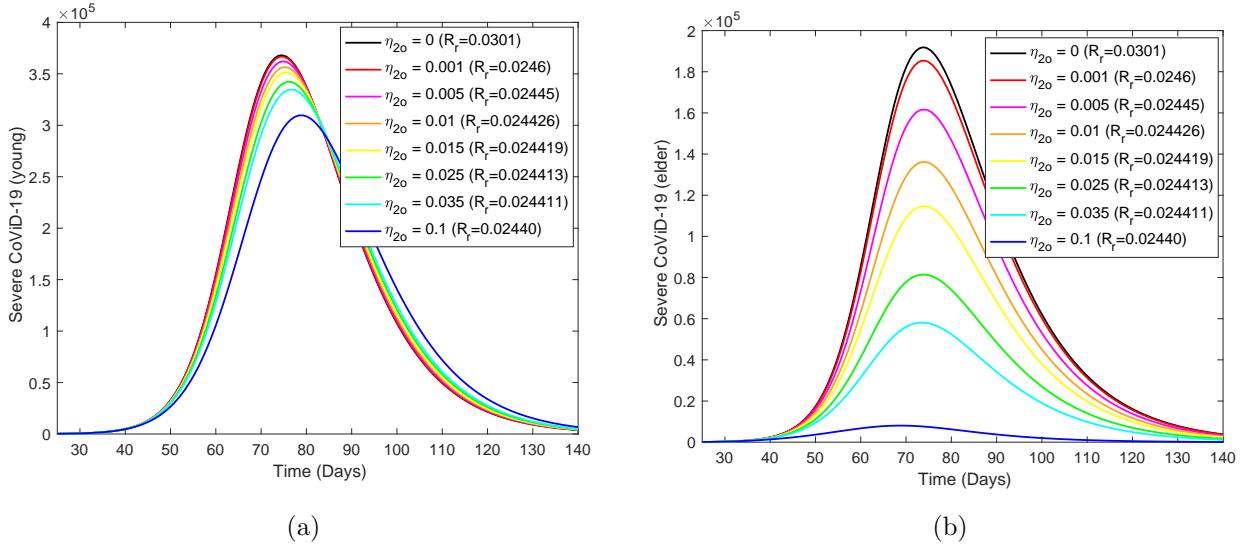


Figure 19: The curves of severe cases of CoViD-19 D_{2j} , $j = y, o$, varying η_{2o} , fixing $\eta_{2y} = 0.01 \text{ days}^{-1}$. Curves from top to bottom corresponds to increasing η_2 . The beginning of isolation is at $t = 27$.

$\eta_{2o} = 0.015$, $\eta_{2o} = 0.035$ and $\eta_{2o} = 0.1 \text{ (days}^{-1})$. Values for Ω , Π , S^{is} and I , for $\eta_{2o} = \eta_{2y} = 0$, are those used in Table 3, as well as the definitions of the percentages.

Figures 19 and 20 and Table 4 portrait preferential isolation of elder persons, but maintaining young persons isolated at a fixed level. Hence, the increasing in η_{2o} of course protects elder persons, but young persons are also benefitted.

Tables 3 and 4 show two kinds isolation for two different goals. If the objective is diminishing

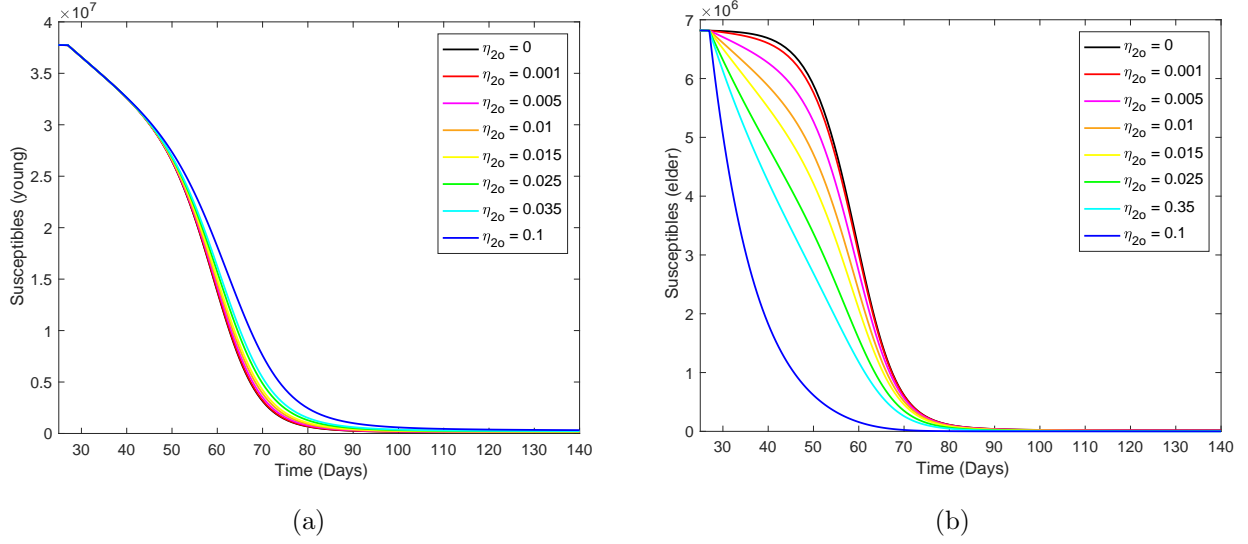


Figure 20: The curves of the number of susceptible persons S_j , $j = y, o$, varying η_{2o} , fixing $\eta_{2y} = 0.01 \text{ days}^{-1}$. Curves from top to bottom corresponds to decreasing η_{2o} . The beginning of isolation is at $t = 27$.

Table 4: Values and percentages of Ω , Π , Q and I fixing $\eta_{2y} = 0.01 \text{ days}^{-1}$ and varying $\eta_{2o} = 0.015$, $\eta_{2o} = 0.035$ and $\eta_{2o} = 0.1 \text{ (days}^{-1})$. y , o and Σ stand for, respectively, young, elder and total persons.

	$\eta_{2o} = 0.015$			$\eta_{2o} = 0.035$			$\eta_{2o} = 0.1$		
	y	o	Σ	y	o	Σ	y	o	Σ
Ω (10^6)	1.272	0.3452	1.6172	1.251	0.1802	1.4312	1.216	0.0274	1.2434
Π	11300	38350	49650	11110	20030	31140	10840	3050	13890
S (10^5)	1.787	0.05501	1.84201	2.347	0.00943	2.35643	3.288	0.0002	3.2882
Q (10^7)	1.101	0.2636	1.3646	1.138	0.4642	1.6022	1.202	0.6498	1.8518
I (10^7)	2.659	0.412	3.071	2.615	0.2151	2.8301	2.539	0.0327	2.5717
Ω (%)	70.75	61.31	68.50	69.58	32.01	60.62	67.63	4.87	52.66
Π (%)	70.63	61.21	63.13	69.44	31.97	39.59	67.75	4.87	17.66
S (%)	144.2	223.4	145.8	189.4	38.3	186.5	265.4	0.81	260.22
Q (%)	29.14	38.65	30.60	30.12	68.06	35.92	31.82	95.28	41.52
I (%)	70.68	6.13	69.26	69.51	3.20	63.82	67.49	0.49	58.00

the total number of severe CoViD-19 cases Ω , the better strategy is isolating more young than elder persons. However, if the goal is the reduction of fatality cases Π , the better strategy is the isolating more elder than young persons, but if the isolation is very intense ($\eta_{2y} = \eta_{2o} = 0.1$), then isolating more young persons is recommended. Notice that only strategy $\eta_{2o} = 0.01$ and $\eta_{2y} = 0.1$ attains the number of isolated susceptible persons above the threshold 3.815×10^7 .

3.2.2 Scenarios – Isolation and releasing

When releasing is introduced, then equation (9) is not anymore valid to evaluated the accumulated number of isolated susceptible persons. Hence, we use Q_y , Q_o and $Q = Q_y + Q_o$ for the numbers of isolated susceptible, respectively, young, elder and total persons. Q_y and Q_o are solutions of the system of equations (2), (3) and (4).

At $t = 0$ (February 26) the first case of severe CiViD-19 was confirmed, and at $t = 27$ (March 24) isolation as mechanism of control (described by η_{2y} and η_{2o}) was introduced until April 22.² Hence, the beginning of releasing of isolated persons will occur at the simulation time $t = 56$.³ We assume that same rates of releasing are applied to young and elder persons, that is, $\eta_3 = \eta_{3y} = \eta_{3o}$, and consider regime 1-type isolation, that is, $\eta_2 = \eta_{2o} = \eta_{2y}$. Hence, from time 0 to 27 we have $R_0 = 6.915$ (no isolation), we have regime 1-type isolation from 27 to 56 with $R_r = 0.007$, and sinceafter 56, we have isolation and releasing with value of R_r depending on η_3 .

In order to assess epidemiological scenarios when isolated persons are released, we fix $\eta_2 = 0.035$ ($days^{-1}$), and vary $\eta_3 = 0$ ($R_r = 0.007$), 0.0055 ($R_r = 0.84$), 0.01 ($R_r = 1.49$), 0.015 ($R_r = 2.02$), 0.25 ($R_r = 2.82$), 0.035 ($R_r = 3.39$) and 0.1 ($R_r = 5.07$). The value for the reduced reproduction number is R_r is calculated from equation (10).

Figure 21 shows curves of severe cases of CoViD-19 D_{2j} , $j = y, o$, fixing $\eta_2 = 0.035$ $days^{-1}$, and varying η_3 . The beginning of release is at $t = 56$, date proposed by the São Paulo State authorities. For instance, when $\eta_3 = 0.035$ $days^{-1}$, the peaks are for young and elder persons, respectively, 2.31×10^5 and 9.06×10^4 , which occur at $t = 99$ and $t = 98$.

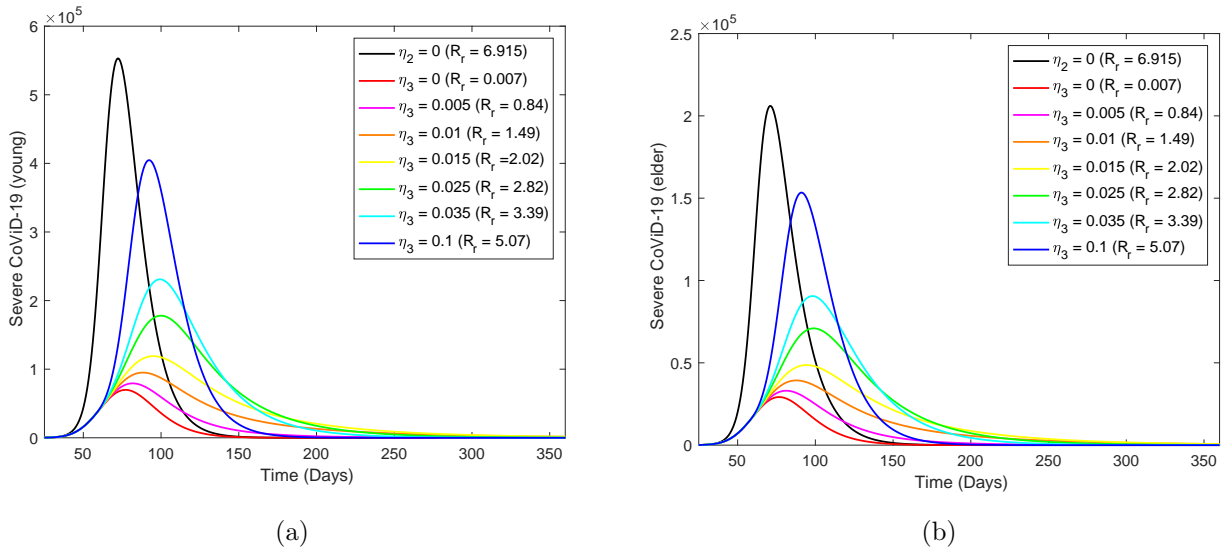


Figure 21: The curves of severe cases of CoViD-19 D_{2j} , $j = y, o$, fixing $\eta_2 = 0.035$ $days^{-1}$, and varying η_3 . Curves from top to bottom corresponds to decreasing η_3 . The beginning of release is at $t = 56$.

²In April 6 the isolation was extended until April 22.

³Simulations were done in April 10.

The curves of accumulated cases of severe CoViD-19 Ω , accumulated cases of CoViD-19 deaths Π , the number of isolated susceptible person S^{is} , and the number of immune persons I are similar than those shown in foregoing section. For this reason, we present in Table 5 ($\eta_2 = 0.035 \text{ days}^{-1}$ fixed) their values at $t = 360$ for young, elder and all persons, letting $\eta_{3o} = 0.015$, $\eta_{3o} = 0.035$ and $\eta_{3o} = 0.1 \text{ (days}^{-1}\text{)}$. Values for Ω , Π , S^{is} and I , for $\eta_2 = 0$, are those used in Table 3, as well as the definitions of the percentages.

Table 5: Values and percentages of Ω , Π , Q and I fixing $\eta_{2y} = \eta_{2o} = 0.035 \text{ days}^{-1}$ and varying $\eta_3 = 0.015$, $\eta_3 = 0.035$ and $\eta_3 = 0.1 \text{ (days}^{-1}\text{)}$. y , o and Σ stand for, respectively, young, elder and total persons. Releasing initiates at $t = 56$.

	$\eta_3 = 0.015$			$\eta_3 = 0.035$			$\eta_3 = 0.1$		
	y	o	Σ	y	o	Σ	y	o	Σ
$\Omega \text{ (} 10^6 \text{)}$	1.121	0.3723	1.4933	1.531	0.4927	2.0237	1.75	0.552	2.302
Π	9985	41570	51555	13650	55110	68760	15600	61720	77320
$S \text{ (} 10^6 \text{)}$	4.317	0.676	4.993	3.012	0.422	3.434	1.098	0.1004	1.198
$Q \text{ (} 10^7 \text{)}$	1.016	0.161	1.177	0.299	0.0422	0.3412	0.0381	0.0035	0.0416
$I \text{ (} 10^7 \text{)}$	2.331	0.442	2.773	3.183	0.585	3.768	3.636	0.655	4.291
$\Omega \text{ (\%)}$	62.35	66.13	63.25	85.15	87.51	85.71	97.33	98.01	97.49
$\Pi \text{ (\%)}$	62.41	66.35	65.55	85.31	87.96	87.43	97.50	98.52	98.31
$S \text{ (\%)}$	3484	27446	3951	2431	17133	2717	886	4076	948
$Q \text{ (\%)}$	26.89	23.61	26.39	7.91	6.19	7.65	1.01	0.51	0.93
$I \text{ (\%)}$	61.96	6.57	62.54	84.61	8.70	84.97	96.65	9.74	96.77

Figure 22 shows curves of severe cases of CoViD-19 D_{2j} , $j = y, o$, fixing $\eta_2 = 0.035 \text{ days}^{-1}$, and varying η_3 . The beginning of release is at $t = 49$, a week earlier. For instance, when $\eta_3 = 0.035 \text{ days}^{-1}$, the peaks are for young and elder persons, respectively, 2.515×10^5 and 9.827×10^4 , which occur at $t = 93$ and 92 . In comparison with Figure 21, the peaks are increased for young and elder persons in, respectively, 8.9% and 8.5%, which are both anticipated in 6 days.

The curves of accumulated cases of severe CoViD-19 Ω , accumulated cases of CoViD-19 deaths Π , the number of isolated susceptible person S^{is} , and the number of immune persons I are similar than those shown in foregoing section. For this reason, we present in Table 6 ($\eta_2 = 0.035 \text{ days}^{-1}$ fixed) their values at $t = 360$ for young, elder and all persons, letting $\eta_{3o} = 0.015$, $\eta_{3o} = 0.035$ and $\eta_{3o} = 0.1 \text{ (days}^{-1}\text{)}$. Values for Ω , Π , S^{is} and I , for $\eta_2 = 0$, are those used in Table 3, as well as the definitions of the percentages.

Figure 23 shows curves of severe cases of CoViD-19 D_{2j} , $j = y, o$, fixing $\eta_2 = 0.035 \text{ days}^{-1}$, and varying η_3 . The beginning of release is at $t = 63$, a week later. For instance, when $\eta_3 = 0.035 \text{ days}^{-1}$, the peaks are for young and elder persons, respectively, 2.084×10^5 and 8.197×10^4 , which occur at $t = 108$ and 107 . In comparison with Figure 21, the peaks are decreased for young and elder persons in, respectively, 9.8% and 9.5%, which are both delayed in 9 days.

The curves of accumulated cases of severe CoViD-19 Ω , accumulated cases of CoViD-19 deaths Π , the number of isolated susceptible person S^{is} , and the number of immune persons

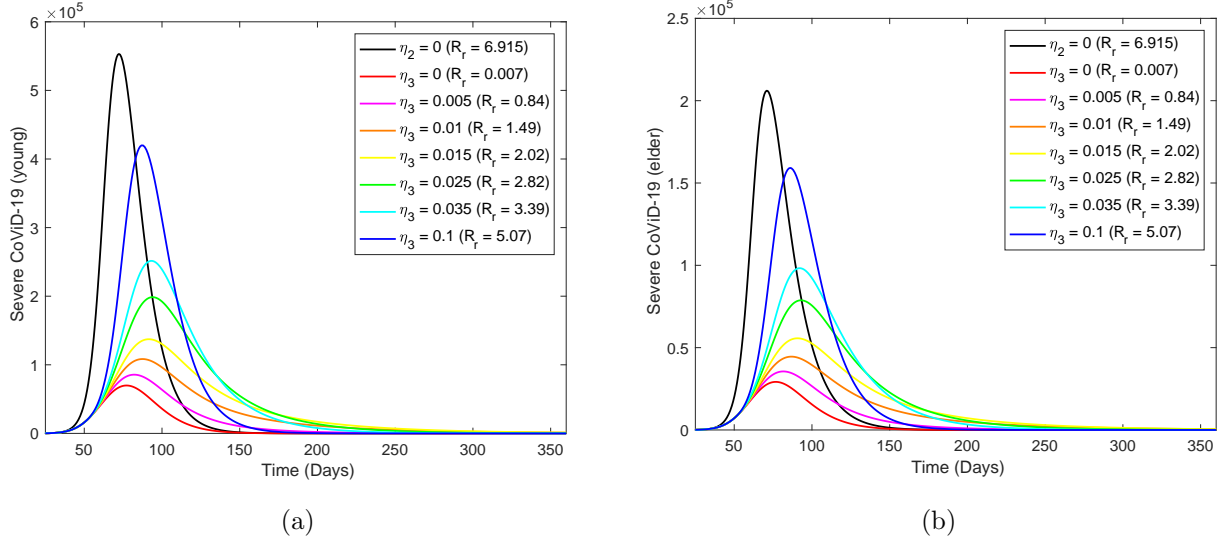


Figure 22: The curves of severe cases of CoViD-19 D_{2j} , $j = y, o$, fixing $\eta_2 = 0.035 \text{ days}^{-1}$, and varying η_3 . Curves from top to bottom corresponds to decreasing η_3 . The beginning of release is at $t = 49$.

Table 6: Values and percentages of Ω , Π , Q and I fixing $\eta_{2y} = 0.01 \text{ days}^{-1}$ and varying $\eta_{2o} = 0.015$, $\eta_{2o} = 0.035$ and $\eta_{2o} = 0.1 \text{ (days}^{-1})$. y , o and Σ stand for, respectively, young, elder and total persons. Releasing initiates at $t = 49$.

	$\eta_3 = 0.015$			$\eta_3 = 0.035$			$\eta_3 = 0.1$		
	y	o	Σ	y	o	Σ	y	o	Σ
$\Omega (10^6)$	1.131	0.3748	1.5058	1.535	0.4937	2.0287	1.751	0.5523	2.3
Π	10080	41870	51950	13690	55220	68910	15620	61770	77390
$S (10^6)$	4.271	0.67	4.941	2.971	0.4166	3.3876	1.074	0.0967	1.17
$Q (10^7)$	1.001	0.158	1.159	0.2949	0.042	0.3369	0.037	0.0034	0.04
$I (10^7)$	2.352	0.445	2.797	3.191	0.586	3.777	3.639	0.656	4.295
$\Omega (\%)$	62.90	66.57	63.78	85.37	87.69	85.93	97.39	98.10	97.56
$\Pi (\%)$	63.00	66.83	66.05	85.56	88.14	87.62	97.63	98.60	98.40
$S (\%)$	3447	27203	3910	2398	16914	2681	867	3926	926
$Q (\%)$	26.50	23.17	25.99	7.81	6.16	7.55	0.98	0.50	0.91
$I (\%)$	62.52	6.62	63.08	84.82	8.72	85.18	96.73	9.76	96.86

I are similar than those shown in foregoing section. For this reason, we present in Table 7 ($\eta_2 = 0.035 \text{ days}^{-1}$ fixed) their values at $t = 360$ for young, elder and all persons, letting $\eta_{3o} = 0.015$, $\eta_{3o} = 0.035$ and $\eta_{3o} = 0.1 \text{ (days}^{-1})$. Values for Ω , Π , S^{is} and I , for $\eta_2 = 0$, are those used in Table 3, as well as the definitions of the percentages.

Comparing Figures 21, 22 and 23, the peaks are increased in 9% and anticipated in 6 days if isolation is released 7 days earlier, while the peaks are decreased in 10% and delayed in 9 days

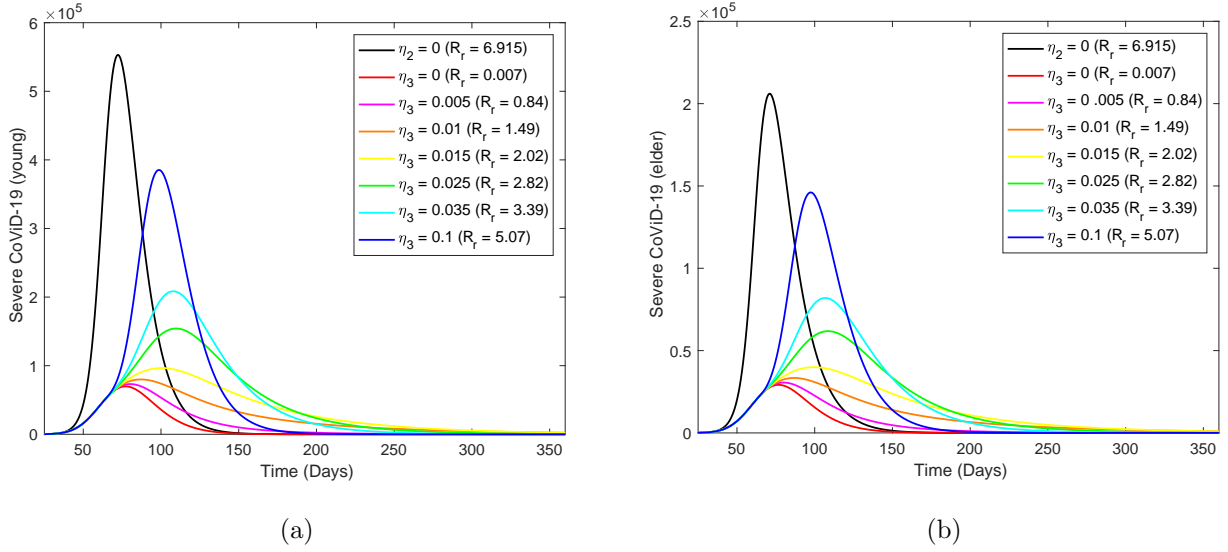


Figure 23: The curves of severe cases of CoViD-19 D_{2j} , $j = y, o$, fixing $\eta_2 = 0.035 \text{ days}^{-1}$, and varying η_3 . Curves from top to bottom corresponds to decreasing η_3 . The beginning of release is at $t = 63$.

Table 7: Values and percentages of Ω , Π , Q and I fixing $\eta_{2y} = 0.01 \text{ days}^{-1}$ and varying $\eta_{2o} = 0.015$, $\eta_{2o} = 0.035$ and $\eta_{2o} = 0.1 \text{ (days}^{-1})$. y , o and Σ stand for, respectively, young, elder and total persons. Releasing initiates at $t = 63$.

	$\eta_3 = 0.015$			$\eta_3 = 0.035$			$\eta_3 = 0.1$		
	y	o	Σ	y	o	Σ	y	o	Σ
$\Omega (10^6)$	1.111	0.37	1.481	1.527	0.49	2.017	1.747	0.55	2.297
Π	9885	41260	51145	13620	55020	68640	15580	61660	77240
$S (10^6)$	4.358	0.68	5.038	3.045	0.43	3.475	1.126	0.105	1.231
$Q (10^7)$	1.032	0.162	1.194	0.3024	0.043	0.3454	0.039	0.0037	0.0427
$I (10^7)$	2.309	0.439	2.748	3.176	0.585	3.761	3.632	0.655	4.287
$\Omega (\%)$	61.79	65.72	62.73	84.93	87.03	85.43	97.16	97.69	97.29
$\Pi (\%)$	61.78	65.86	65.03	85.13	87.82	87.27	97.38	98.42	98.21
$S (\%)$	3517	27609	3987	2458	17458	2750	909	4263	974
$Q (\%)$	27.32	23.75	26.77	8.00	6.30	7.74	1.03	0.54	0.96
$I (\%)$	61.38	6.53	61.97	84.42	8.70	84.82	96.54	9.74	96.68

if isolation is released 7 days later. From Tables 5, 6 and 7, the increase in severe coViD-19 cases and deaths due to this disease by anticipating isolation in 7 days are 0.9%, 0.3% and 0.06% for, respectively, $\eta_3 = 0.015$, 0.035 and 0.1 (days^{-1}); while by delaying in 7 days, both are decreased in 0.9%, 0.6% and 0.2% for, respectively, $\eta_3 = 0.015$, 0.035 and 0.1 (days^{-1}). However, 0.9% represents 95 deaths.

In Figure 24 we show releasing occurring without isolation, that is, from time 0 to 27, we

have $R_0 = 6.915$ (no isolation), we have regime 1-type isolation from 27 to 56, $R_r = 0.007$, and sinceafter 56, we have only releasing with $R_0 = 6.915$ ($\eta_2 = 0$ and $\eta_3 = 0.035 \text{ days}^{-1}$).

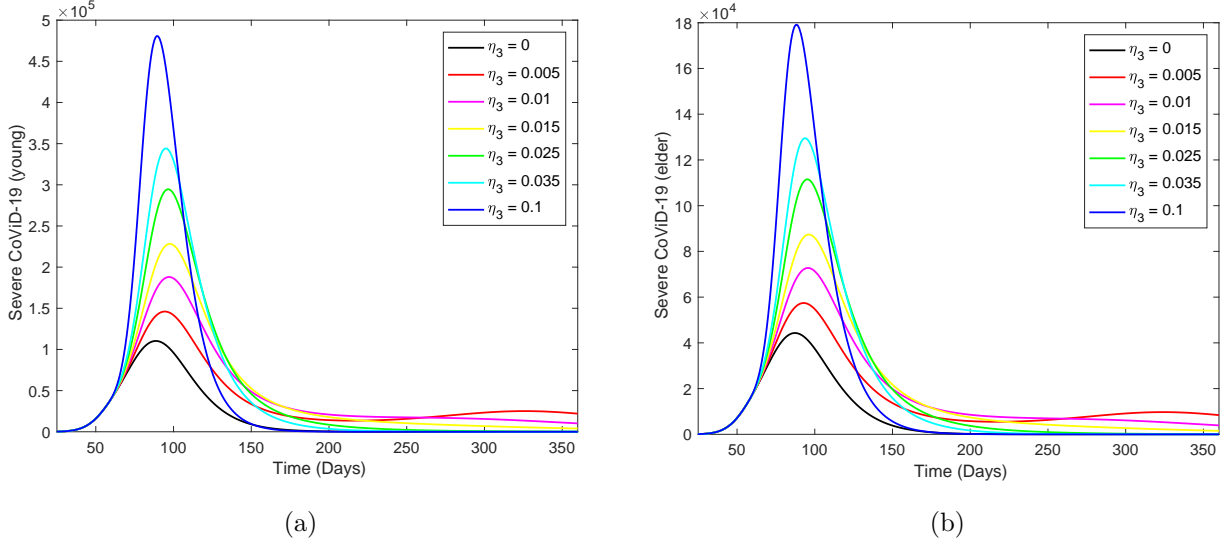


Figure 24: The curves of severe cases of CoViD-19 D_{2j} , $j = y, o$, letting $\eta_2 = 0.035$ and $\eta_3 = 0$ (days^{-1}) during isolation, and $\eta_2 = 0$ and $\eta_3 = 0.035$ (days^{-1}) when releasing begins at $t = 56$. Curves from top to bottom corresponds to decreasing η_3 .

When releasing is done without new isolations, there appears small epidemics (see curve for $\eta_3 = 0.005$), which is delayed as η_3 increases (for other values, the second small epidemics does not appear until 360 days). If releasing strategy is done, the first wave does not vanish completely, except for huge releasing scheme (higher η_3). This is a good epidemiological scenario due to not only in the diminishing in the pressure for hospitalization (consequently, decreases deaths), but also in the increasing in immune persons, hence decreasing the effective reproduction number (known as herd immunity).

4 Discussion

System of equations (2), (3) and (4) were simulated to providing epidemiological scenarios. These scenarios are more reliable if based on credible values assigned to model parameters. We used ratio 4 : 1 for the ratios of asymptomatic:symptomatic and mild:severe (non-hospitalized:hospitalized) CoViD-19 [2]. Also, we let $\alpha_y = 0.1\alpha_o$, and α_o must be such that deaths will occur in 10% of hospitalized elder persons, hence, 1% of hospitalized young persons will die [9]. We used overvalued parameters, except maybe the ratio between asymptomatic:symptomatic, which is completely unknown. In many viruses, the ratio is higher than 4 : 1, but for new coronavirus is unknown. When mass testing against new coronavirus could be done, then this ratio can be estimated.

The least square estimation method was approximated by the sum of the square of the distance between parametrized curve and observed data. When estimation of epidemic curves

are based on few available data, in general parameters are overestimated. Hence, both transmission and mortality rates were overestimated. Fortunately, there was another information to use: 10% of fatality among elder hospitalized persons. Taking into account this information, we estimated lower mortality rates, but estimated transmission rates were those based on few available data. Hence, the basic reproduction number $R_0 = 6.915$ seems overestimated.

Let us consider estimation of transmission and mortality rates based on few data. From Figures 7 and 8, it is expected at the end of the first wave of epidemics, 2.36 million of severe (hospitalized) CoViD-19 cases, and 250 thousand of deaths due to this disease in the São Paulo State. If we consider a 5-times higher inhabitants than the São Paulo State, it is expected 11.8 million of severe (hospitalized) CoViD-19 cases, and 1,250 thousand of deaths. Approximately these numbers of cases and deaths were projected to Brazil by Ferguson *et al.* [4]. However, the second method of estimation for fatality rates resulted in 78.7 thousand of deaths in the São Paulo State, but the number of severe cases is the same. Hence, extrapolating to Brazil, the number is 383 thousand of deaths.

We address the question of the discrepancy in providing number of deaths during the first wave of epidemics. Mathematical and computational (especially agent based models) models that are based on data to estimate model parameters, these models must be fed continuously with new data and reestimated model parameters. As the number of data increases, their estimations become more and more reliable. Hence, initial estimations and forecasting are extremely bad, and, moreover, they become dangerous when predicting catastrophic scenarios, which can lead to formulate mistaken public health policies.

With respect to isolation of susceptible persons, depending on the target we have two strategies. If the goal is decreasing the number of CoViD-19 cases in order to adequate capacity of Hospital and ICU, the better strategy is isolating more young than elder persons. However, if death due to CoViD-19 is the main goal, better strategy is isolating more elder than young persons.

We also studied releasing strategies. We compare the releasing that will be initiated in April 22, with releasing one week earlier (April 19) and one week later (April 29).

The estimated basic reproduction number and its partial values were $R_0 = 6.915$ (partials $R_{0y} = 5.606$ and $R_{0o} = 1.309$), and the asymptotic fraction of susceptible persons and its partial fractions provided by Runge-Kutta method were $s^* = 0.15008$, $s_y^* = 0.14660$ and $s_o^* = 0.00348$. Using equation (A.10), we obtain $1/R_0 = 0.1446$. Clearly, s^* is not the inverse of the basic reproduction number R_0 , and $f(s^*, s_y^*, s_o^*)$ in equation (A.10) is not $s^* = s_y^* + s_o^*$, neither $R_{0y}s_y^* + R_{0o}s_o^*$. The analysis of the non-trivial equilibrium point to find $f(s^*, s_y^*, s_o^*)$ is left to a further work. In order to understand this question, we suppose that new coronavirus is circulating in non-communicating young and elder sub-populations, then each population approach to $s_y^* = 1/R_{0y} = 0.178$ or $s_o^* = 1/R_{0o} = 0.764$ at steady state (non-trivial equilibrium point P^*). But, new coronavirus is circulating in a homogeneously mixed populations of young and elder persons (this is a strong assumption of the modeling). Using equation (1), let us calculate the forces of infection $\lambda_1 = \beta_{1y}A_y + \beta_{2y}D_{1y}$ (contribution due to infectious young persons), $\lambda_2 = \beta_{1o}A_o + \beta_{2o}D_{1o}$ (elder persons) and $\lambda = \lambda_1 + \lambda_2$ (both classes), which are shown in Figure 25 (λ is the force of infection acting on young persons, and for elder persons, it is enough multiplying by the factor ψ).

The peaks of the force of infection for λ_1 , λ_2 and λ are, respectively, 8.62×10^6 , 1.69×10^6

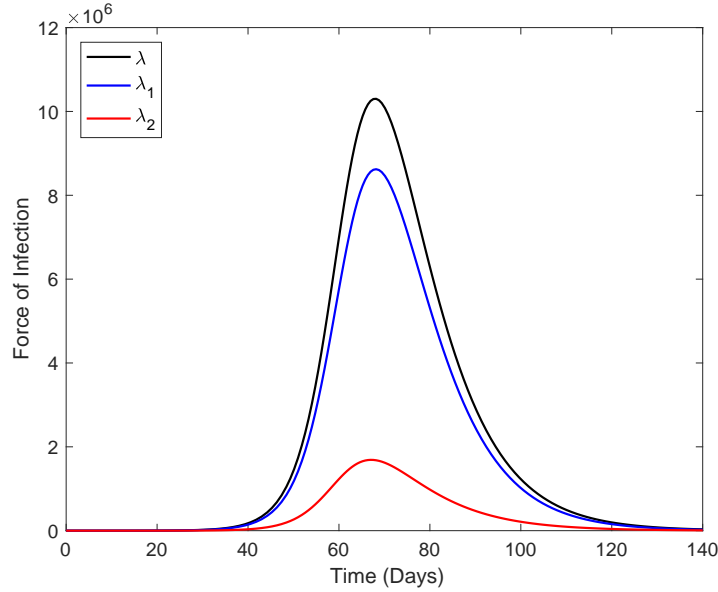


Figure 25: The forces of infection $\lambda_1 = \beta_{1y}A_y + \beta_{2y}D_{1y}$ (young persons), $\lambda_2 = \beta_{1o}A_o + \beta_{2o}D_{1o}$ (elder persons) and $\lambda = \lambda_1 + \lambda_2$ (both classes).

and 10.31×10^6 , which occur at 68.18, 66.94 and 68.18 (days), and contributions at peak of λ_1 and λ_2 with respect to λ are 83.6% and 16.4%. The ratio between peaks $\lambda_1:\lambda_2$ is 5.1:1, which is close to the ratio between numbers of young:elder 5.5:1. When virus circulates in mixed populations, young and elder persons are infected additionally by, respectively, elder (λ_2) and young (λ_1) persons. This is the reason for the actual equilibrium values are bigger ($s_y^* > 1/R_{0y}$ and $s_o^* > R_{0o}$), but among elder persons the increase (220-times) is huge (λ_1 , very big, acting in relatively small population S_o). For this reason contacts between elder and young persons must be avoided.

5 Conclusion

We formulated a mathematical model considering two subpopulations comprised by young and elder persons to study CoViD-19 in the São Paulo State, Brazil. The model considered continuous but constant rates of isolation and releasing. In a future work, we change rates to describe isolation and releasing by proportions of susceptible persons being isolated or released. The reason behind this is the absence of translation of rates to proportions.

Our model estimated quite same number of severe CoViD-19 cases predicted by Ferguson *et al.* [4] for Brazil, but 3.3-times lower for deaths due to CoViD-19. The difference is mainly done by estimation of the additional mortality rates. It is also expected that R_0 must be lower if additional information may exist, or more data will be available. As consequence, maybe severe CoViD019 cases should be much lower (consequently, deaths also). If currently adopted lockdown is indeed based on the goal of decreasing hospitalized CoViD-19 cases, then our model agrees, since it predicts that higher number of young and elder persons must be isolated

in order to achieve this objective. However, if the goal is reduction in the number of deaths due to CoViD-19, as much elder persons must be isolated, but not so much young persons. Remember that in a mixing of young and elder persons, the infection is much harmful in elder than young persons, which is reason to avoid contact between them. An optimal rates of isolation of young and elder persons to reduce both CoViD-19 cases and deaths can be obtained by optimal control theory [8].

If vaccine and efficient treatments are available, the pandemic of new coronavirus should not be considered a threaten to public health. However, currently, there is not vaccine, neither efficient treatment. For this reason the adoption of isolation or lockdown is a recommended strategy, which can be less hardly implemented if there is enough kit to test against new coronavirus. Remember that all isolation strategies considered in our model assume the identification of susceptible persons. Hence isolation as control mechanism allows an additional time to seek for cure (medicine) and/or develop vaccine.

References

- [1] R.M. Anderson, R.M. May, R.M., Infectious Diseases of Human. Dynamics and Control, Oxford University Press, Oxford, New York, Tokyo (1991).
- [2] Boletim Epidemiológico 08 (April 9, 2020), <https://www.saude.gov.br/images/pdf/2020/April/09/be-covid-08-final-2.pdf>.
- [3] O. Diekmann, J.A.P. Heesterbeek, M.G. Roberts, The construction of next-generation matrices for compartmental epidemic models, *J. R. Soc. Interface* 7 (2010) 873-885.
- [4] N.M. Ferguson *et al.*, Impact of non-pharmaceutical interventions (NPIs) to reduce COVID-19 mortality and healthcare demand, Imperial College COVID-19 Response Team (2020).
- [5] R.Y. Li, *et al.*, Substantial undocumented infection facilitates the rapid dissemination of novel coronavirus (SARS-CoV2), *Science* 16 Mar (2020) eabb3221.
- [6] SEADE – Fundação Sistema Estadual, <https://www.seade.gov.br> (2020).
- [7] Z. Shuai, P. van den Driessche, Global stability of infectious disease model using Lyapunov functions, *SIAM J. App. Math.* 73(4) (2013) 1513-1532.
- [8] R.C.A. Thomé, H.M. Yang, L. Eesteva, Optimal control of *Aedes aegypti* mosquitoes by the sterile insect technique and insecticide, *Mathematical Biosciences* (223) (2009) 12-23.
- [9] WHO, Report of the WHO-China Joint Mission on Coronavirus Disease 2019 (COVID-19), 16-24 February 2020 (2020).
- [10] H.M. Yang, Modelling vaccination strategy against directly transmitted diseases using a series of pulses, *Journal of Biological Systems* (6)(2) (1998) 187-212.

- [11] H.M. Yang, Directly transmitted infections modeling considering age-structured contact rate – Epidemiological analysis, *Mathematical and Computer Modelling* 29(7) (1999) 11-30.
- [12] H.M. Yang, Directly transmitted infections modeling considering age-structured contact rate, *Mathematical and Computer Modelling*, 29(8) (1999) 39-48.
- [13] H.M. Yang, Modeling directly transmitted infections in a routinely vaccinated population – The force of infection described by Volterra integral equation, *Applied Mathematics and Computation* (122)(1) (2001) 27-58.
- [14] S.M. Raimundo, H.M. Yang, R.C. Bassanezi, M.A.C. Ferreira, The attracting basins and the assessment of the transmission coefficients for HIV and *M. tuberculosis* infections among women inmates, *Journal of Biological Systems* (10)(1) (2002) 61-83.
- [15] H.M. Yang, The basic reproduction number obtained from Jacobian and next generation matrices – A case study of dengue transmission modelling, *BioSystems* 126 (2014) 52-75.
- [16] H.M. Yang, D. Greenhalgh, Proof of conjecture in: The basic reproduction number obtained from Jacobian and next generation matrices – A case study of dengue transmission modelling, *Appl. Math. Comput.* 265 (2015) 103-107.
- [17] H.M. Yang, J.L. Boldrini, A.C. Fassoni, K.K.B. Lima, L.S.F. Freitas, M.C. Gomez, V.F. Andrade, A.R.R. Freitas, Fitting the incidence data from the City of Campinas, Brazil, based on dengue transmission modellings considering time-dependent entomological parameters, *PlosOne* (March 24) (2016) 1-41.
- [18] H.M. Yang, The transovarial transmission un the dynamics of dengue infection: Epidemiological implications and thresholds, *Math. Biosc.* 286 (2017) 1-15.
- [19] H.M. Yang, Are the beginning and ending phases of epidemics provided by next generation matrices? – Revisiting drug sensitive and resistant tuberculosis model, *Appl. Math. Comput.* submitted (2020).

A Trivial equilibrium and its stability

By the fact that N is varying, the system is non-autonomous non-linear differential equations. To obtain autonomous system of equations, we use fractions of individuals in each compartment, defined by, with $j = y$ and o ,

$$x_j = \frac{X_j}{N}, \quad \text{where } X = S_j, Q_j, E_j, A_j, Q_{1j}, D_{1j}, Q_{2j}, D_{2j}, I,$$

resulting in

$$\frac{d}{dt}x_j \equiv \frac{d}{dt}\frac{X_j}{N} = \frac{1}{N}\frac{d}{dt}X_j - x_j\frac{1}{N}\frac{d}{dt}N = \frac{1}{N}\frac{d}{dt}X_j - x(\phi - \mu) + x_j(\alpha_y d_{2y} + \alpha_o d_{2o}),$$

using equation (5) for N . Hence, equations (2), (3) and (4) in terms of fractions become, for susceptible persons,

$$\begin{cases} \frac{d}{dt}s_y &= \phi - (\eta_{2y} + \varphi + \phi) s_y - \lambda s_y + \eta_{3y}q_y + s_y (\alpha_y d_{2y} + \alpha_o d_{2o}) \\ \frac{d}{dt}s_o &= \varphi s_y - (\eta_{2o} + \phi) s_o - \lambda \psi s_o + \eta_{3o}q_o + s_o (\alpha_y d_{2y} + \alpha_o d_{2o}), \end{cases} \quad (\text{A.1})$$

for infected persons,

$$\begin{cases} \frac{d}{dt}q_j &= \eta_{2j}s_j - (\eta_{3j} + \phi) q_j + q_j (\alpha_y d_{2y} + \alpha_o d_{2o}) \\ \frac{d}{dt}e_j &= \lambda (\delta_{jy} + \psi \delta_{jo}) s_j - (\sigma_j + \phi) e_j + e_j (\alpha_y d_{2y} + \alpha_o d_{2o}) \\ \frac{d}{dt}a_j &= p_j \sigma_j e_j - (\gamma_j + \eta_j + \chi_j + \phi) a_j + a_j (\alpha_y d_{2y} + \alpha_o d_{2o}) \\ \frac{d}{dt}q_{1j} &= (\eta_j + \chi_j) a_j - (\gamma_j + \phi) q_{1j} + q_{1j} (\alpha_y d_{2y} + \alpha_o d_{2o}) \\ \frac{d}{dt}d_{1j} &= (1 - p_j) \sigma_j e_j - (\gamma_{1j} + \eta_{1j} + \phi) d_{1j} + d_{1j} (\alpha_y d_{2y} + \alpha_o d_{2o}) \\ \frac{d}{dt}q_{2j} &= (\eta_{1j} + m_j \gamma_{1j}) d_{1j} - (\gamma_j + \xi_j + \phi) q_{2j} + q_{2j} (\alpha_y d_{2y} + \alpha_o d_{2o}) \\ \frac{d}{dt}d_{2j} &= (1 - m_j) \gamma_{1j} d_{1j} + \xi_j q_{2j} - (\gamma_{2j} + \theta_j + \phi + \alpha_j) d_{2j} + d_{2j} (\alpha_y d_{2y} + \alpha_o d_{2o}), \end{cases} \quad (\text{A.2})$$

and for immune persons

$$\frac{d}{dt}i = \gamma_y a_y + \gamma_y q_{1y} + \gamma_y q_{2y} + (\gamma_{2y} + \theta_y) d_{2y} + \gamma_o a_o + \gamma_o q_{1o} + \gamma_o q_{2o} + (\gamma_{2o} + \theta_o) d_{2o} - \phi i + i (\alpha_y d_{2y} + \alpha_o d_{2o}), \quad (\text{A.3})$$

where λ is the force of infection given by equation (1), and

$$\sum_{j=y,o} (s_j + q_j + e_j + a_j + q_{1j} + d_{1j} + q_{2j} + d_{2j}) + i = 1,$$

which is autonomous system of equations. We remember that all classes vary with time, however their fractions attain steady state (the sum of derivatives of all classes is zero). This system of equations is not easy to determine non-trivial (endemic) equilibrium point P^* . Hence, we restrict our analysis with respect to trivial (disease free) equilibrium point.

The trivial or disease free equilibrium P^0 is given by

$$P^0 = (s_j^0, q_j^0, e_j^0 = 0, a_j^0 = 0, q_{1j}^0 = 0, d_{1j}^0 = 0, q_{2j}^0 = 0, d_{2j}^0 = 0, i^0 = 0),$$

for $j = y$ and o , where

$$\begin{cases} s_y^0 = \frac{\phi (\eta_{3y} + \phi)}{\phi (\eta_{2y} + \eta_{3y} + \phi) + \varphi (\eta_{3y} + \phi)} \\ q_y^0 = \frac{\phi \eta_{2y}}{\phi (\eta_{2y} + \eta_{3y} + \phi) + \varphi (\eta_{3y} + \phi)} \\ s_o^0 = \frac{\varphi (\eta_{3y} + \phi) (\eta_{3o} + \phi)}{[\phi (\eta_{2y} + \eta_{3y} + \phi) + \varphi (\eta_{3y} + \phi)] (\eta_{2o} + \eta_{3o} + \phi)} \\ q_o^0 = \frac{\varphi \eta_{2o} (\eta_{3y} + \phi)}{[\phi (\eta_{2y} + \eta_{3y} + \phi) + \varphi (\eta_{3y} + \phi)] (\eta_{2o} + \eta_{3o} + \phi)}, \end{cases} \quad (\text{A.4})$$

with $s_y^0 + q_y^0 + s_o^0 + q_o^0 = 1$.

Due to 17 equations, we do not deal with characteristic equation corresponding to Jacobian matrix evaluated at P^0 , but we apply the next generation matrix theory [3].

The next generation matrix, evaluated at the trivial equilibrium P^0 , is obtained considering the vector of variables $x = (e_y, a_y, d_{1y}, e_o, a_o, d_{1o})$. We apply method proposed in [15] and proved in [16]. There are control mechanisms (isolation), hence we obtain the reduced reproduction number R_r by isolation.

In order to obtain the reduced reproduction number, diagonal matrix V is considered. Hence, the vectors f and v are

$$f^T = \begin{pmatrix} \lambda s_y + e_y (\alpha_y d_{2y} + \alpha_o d_{2o}) \\ p_y \sigma_y e_y + a_y (\alpha_y d_{2y} + \alpha_o d_{2o}) \\ (1 - p_y) \sigma_y e_y + d_{1y} (\alpha_y d_{2y} + \alpha_o d_{2o}) \\ \lambda \psi s_o + e_o (\alpha_y d_{2y} + \alpha_o d_{2o}) \\ p_o \sigma_o e_o + a_o (\alpha_y d_{2y} + \alpha_o d_{2o}) \\ (1 - p_o) \sigma_o e_o + d_{1o} (\alpha_y d_{2y} + \alpha_o d_{2o}) \end{pmatrix} \quad (\text{A.5})$$

and

$$v^T = \begin{pmatrix} (\sigma_y + \phi) e_y \\ (\gamma_y + \eta_y + \chi_y + \phi) a_y \\ (\gamma_{1y} + \eta_{1y} + \phi) d_{1y} \\ (\sigma_o + \phi) e_o \\ (\gamma_o + \eta_o + \chi_o + \phi) a_o \\ (\gamma_{1o} + \eta_{1o} + \phi) d_{1o} \end{pmatrix}, \quad (\text{A.6})$$

where the superscript T stands for the transposition of a matrix, from which we obtain the matrices F and V (see [3]) evaluated at the trivial equilibrium P^0 , which were omitted. The next generation matrix FV^{-1} is

$$FV^{-1} = \begin{bmatrix} 0 & \frac{\beta_{1y} s_y^0}{\gamma_y + \eta_y + \chi_y + \phi} & \frac{\beta_{2y} s_y^0}{\gamma_{1y} + \eta_{1y} + \phi} & 0 & \frac{\beta_{1o} s_y^0}{\gamma_o + \eta_o + \chi_o + \phi} & \frac{\beta_{2o} s_y^0}{\gamma_{1o} + \eta_{1o} + \phi} \\ \frac{p_y \sigma_y}{\sigma_y + \phi} & 0 & 0 & 0 & 0 & 0 \\ \frac{(1-p_y) \sigma_y}{\sigma_y + \phi} & 0 & 0 & 0 & 0 & 0 \\ 0 & \frac{\beta_{1y} \psi s_o^0}{\gamma_y + \eta_y + \chi_y + \phi} & \frac{\beta_{2y} \psi s_o^0}{\gamma_{1y} + \eta_{1y} + \phi} & 0 & \frac{\beta_{1o} \psi s_o^0}{\gamma_o + \eta_o + \chi_o + \phi} & \frac{\beta_{2o} \psi s_o^0}{\gamma_{1o} + \eta_{1o} + \phi} \\ 0 & 0 & 0 & \frac{p_o \sigma_o}{\sigma_o + \phi} & 0 & 0 \\ 0 & 0 & 0 & \frac{(1-p_o) \sigma_o}{\sigma_o + \phi} & 0 & 0 \end{bmatrix},$$

and the characteristic equation corresponding to FV^{-1} is

$$\lambda^4 (\lambda^2 - R_r) = 0, \quad (\text{A.7})$$

where the reduced reproduction number R_r and its partial reduced reproduction numbers R_{ry} and R_{ro} are

$$R_r = R_{ry} + R_{ro}, \quad \text{where} \quad \begin{cases} R_{ry} = R_{0y} s_y^0 \\ R_{ro} = R_{0o} \psi s_o^0, \end{cases} \quad \text{with} \quad \begin{cases} R_{0y} = p_y R_{0y}^1 + (1 - p_y) R_{0y}^2 \\ R_{0o} = p_o R_{0o}^1 + (1 - p_o) R_{0o}^2, \end{cases} \quad (\text{A.8})$$

and R_{0y} and R_{0o} are the basic partial reproduction numbers defined by

$$\left\{ \begin{array}{l} R_{0y}^1 = \frac{\sigma_y}{\sigma_y + \phi} \frac{\beta_{1y}}{\gamma_y + \eta_y + \chi_y + \phi}, \quad \text{and} \quad R_{0y}^2 = \frac{\sigma_y}{\sigma_y + \phi} \frac{\beta_{2y}}{\gamma_{1y} + \eta_{1y} + \phi} \\ R_{0o}^1 = \frac{\sigma_o}{\sigma_o + \phi} \frac{\beta_{1o}}{\gamma_o + \eta_o + \chi_o + \phi}, \quad \text{and} \quad R_{0o}^2 = \frac{\sigma_o}{\sigma_o + \phi} \frac{\beta_{2o}}{\gamma_{1o} + \eta_{1o} + \phi}. \end{array} \right. \quad (\text{A.9})$$

Actually, we must have $\eta_j = \chi_j = \eta_{1j} = \chi_{1j} = 0$, with $j = i, o$, to be fit in the definition of the basic reproduction number.

Instead of calculating the spectral radius ($\rho(FV^{-1}) = \sqrt{R_r}$), we apply procedure in [15] (the sum of coefficients of characteristic equation), resulting in a threshold R_r . Hence, the trivial equilibrium point P^0 is locally asymptotically stable (LAS) if $R_r < 1$.

In order to obtain the fraction of susceptible individuals, M must be the simplest (matrix with least number of non-zeros). Hence, the vectors f and v are

$$f^T = \begin{pmatrix} \lambda s_y \\ 0 \\ 0 \\ \lambda \psi s_o \\ 0 \\ 0 \end{pmatrix} \quad \text{and} \quad v^T = \begin{pmatrix} (\sigma_y + \phi) e_y - e_y (\alpha_y d_{2y} + \alpha_o d_{2o}) \\ -p_y \sigma_y e_y + (\gamma_y + \eta_y + \chi_y + \phi) a_y - a_y (\alpha_y d_{2y} + \alpha_o d_{2o}) \\ -(1 - p_y) \sigma_y e_y + (\gamma_{1y} + \eta_{1y} + \phi) d_{1y} - d_{1y} (\alpha_y d_{2y} + \alpha_o d_{2o}) \\ (\sigma_o + \phi) e_o - e_o (\alpha_y d_{2y} + \alpha_o d_{2o}) \\ -p_o \sigma_o e_o + (\gamma_o + \eta_o + \chi_o + \phi) a_o - a_o (\alpha_y d_{2y} + \alpha_o d_{2o}) \\ -(1 - p_o) \sigma_o e_o + (\gamma_{1o} + \eta_{1o} + \phi) d_{1o} - d_{1o} (\alpha_y d_{2y} + \alpha_o d_{2o}) \end{pmatrix},$$

where superscript T stands for the transposition of a matrix, from which we obtain the matrices F and V evaluated at the trivial equilibrium P^0 , which were omitted. The next generation matrix FV^{-1} is

$$FV^{-1} = \begin{bmatrix} R_{0y} s_y^0 & \frac{\beta_{1y} s_y^0}{\gamma_y + \eta_y + \chi_y + \phi} & \frac{\beta_{2y} s_y^0}{\gamma_{1y} + \eta_{1y} + \phi} & R_{0o} s_y^0 & \frac{\beta_{1o} s_y^0}{\gamma_o + \eta_o + \chi_o + \phi} & \frac{\beta_{2o} s_y^0}{\gamma_{1o} + \eta_{1o} + \phi} \\ 0 & 0 & 0 & 0 & 0 & 0 \\ 0 & 0 & 0 & 0 & 0 & 0 \\ R_{0y} \psi s_o^0 & \frac{\beta_{1y} \psi s_o^0}{\gamma_y + \eta_y + \chi_y + \phi} & \frac{\beta_{2y} \psi s_o^0}{\gamma_{1y} + \eta_{1y} + \phi} & R_{0o} \psi s_o^0 & \frac{\beta_{1o} \psi s_o^0}{\gamma_o + \eta_o + \chi_o + \phi} & \frac{\beta_{2o} \psi s_o^0}{\gamma_{1o} + \eta_{1o} + \phi} \\ 0 & 0 & 0 & 0 & 0 & 0 \\ 0 & 0 & 0 & 0 & 0 & 0 \end{bmatrix},$$

and the characteristic equation corresponding to FV^{-1} is

$$\lambda^5 (\lambda - R_r) = 0.$$

The spectral radius is $\rho(FV^{-1}) = R_r = R_{ry} + R_{ro}$ given by equation (A.8). Hence, the trivial equilibrium point P^0 is LAS if $\rho < 1$.

Both procedures resulted in the same threshold, hence, according to [19], the inverse of the reduced reproduction number R_r given by equation (A.8) is a function of the fraction of susceptible individuals at endemic equilibrium s^* through

$$f(s^*, s_y^*, s_o^*) = \frac{1}{R_r} = \frac{1}{R_{ry} + R_{ro}} = \frac{1}{R_{0y} s_y^0 + R_{0o} \psi s_o^0}, \quad (\text{A.10})$$

where $s^* = s_y^* + s_o^*$ (see [18] [19]). For this reason, the effective reproduction number R_e [17], which varies with time, can not be defined by $R_e = R_0 (s_y + \psi s_o)$, or $R_e = R_{0y} s_y + R_{0o} \psi s_o$.

The function $f(\boldsymbol{x})$ is determined by calculating the coordinates of the non-trivial equilibrium point P^* . For instance, for dengue transmission model, $f(s_1^*, s_2^*) = s_1^* \times s_2^*$, where s_1^* and s_2^* are the fractions at equilibrium of, respectively, humans and mosquitoes [18]. For tuberculosis model considering drug-sensitive and resistant strains, there is not $f(\boldsymbol{x})$, but s^* is solution of a second degree polynomial [19].

From equation (A.10), let us assume (or approximate) that $f(s^*, s_y^*, s_o^*) = s_y^* + s_o^*$. Then, we can define the effective reproduction number R_e as

$$R_e = R_r (s_y + s_o), \quad (\text{A.11})$$

which depends on time, and when attains steady state ($R_e = 1$), we have $s^* = 1/R_r$.

When a mechanism of protection of susceptible persons is introduced in a population, the basic reproduction number R_0 is reduced to R_r , the reduced reproduction number. The protection of susceptible persons is done or by vaccine (not yet available), or isolation (or quarantine). The isolation was described by the isolation rate of susceptible persons η_{2j} , with $j = y, o$. When $\eta_{2j} = 0$, the fraction of young persons and elders are, from equation (A.4),

$$\begin{cases} \bar{s}_y^0 = \frac{\phi}{\phi + \varphi} \\ \bar{q}_y^0 = 0 \\ \bar{s}_o^0 = \frac{\varphi}{\phi + \varphi} \\ \bar{q}_o^0 = 0, \end{cases} \quad (\text{A.12})$$

with $\bar{s}_y^0 + \bar{s}_o^0 = 1$, and the reduced reproduction number R_r becomes R_0 , with

$$R_0 = R_{0y} \bar{s}_y^0 + R_{0o} \bar{s}_o^0, \quad (\text{A.13})$$

where R_{0y} and R_{0o} are given by equation (A.9).

The basic partial reproduction number $R_{0y}^1 \bar{s}_y^0$ (or $R_{0y}^2 \bar{s}_o^0$) is the secondary cases produced by one case of asymptomatic individual (or pre-diseased individual) in a completely susceptible young persons without control; and the partial basic reproduction number $R_{0o}^1 \bar{s}_o^0$ (or $R_{0o}^2 \bar{s}_o^0$) is the secondary cases produced by one case of asymptomatic individual (or pre-diseased individual) in a completely susceptible elder persons without control. If all parameters are equal, and $\psi = 1$, then

$$R_0 = [pR_0^1 + (1-p)R_0^2],$$

where $R_0^1 = R_{0y}^1 + R_{0o}^1$ and $R_0^2 = R_{0y}^2 + R_{0o}^2$ are the basic partial reproduction numbers due to asymptomatic and pre-diseased persons.

The global stability follows method proposed in [7]. Let the vector of variables be $x = (e_y, a_y, d_{1y}, e_o, a_o, d_{1o})$, vectors f and v , by equations (A.5) and (A.6), and matrices F and V evaluated from f and v at trivial equilibrium P^0 (omitted here). Vector g , constructed as

$$g^T = (F - V)x^T - f^T - v^T,$$

results in

$$g^T = \begin{pmatrix} \lambda (s_y^0 - s_y) - e_y (\alpha_y d_{2y} + \alpha_o d_{2o}) \\ -a_y (\alpha_y d_{2y} + \alpha_o d_{2o}) \\ -d_{1y} (\alpha_y d_{2y} + \alpha_o d_{2o}) \\ \lambda \psi (s_o^0 - s_o) - e_o (\alpha_y d_{2y} + \alpha_o d_{2o}) \\ -a_o (\alpha_y d_{2y} + \alpha_o d_{2o}) \\ -d_{1o} (\alpha_y d_{2y} + \alpha_o d_{2o}) \end{pmatrix},$$

and $g^T \geq 0$ if $s_y^0 \geq s_y$, $s_o^0 \geq s_o$ and $\alpha_y = \alpha_o = 0$.

Let $v_l = (z_1, z_2, z_3, z_4, z_5, z_6)$ be the left eigenvector satisfying $v_l V^{-1} F = \rho v_l$, where $\rho = \sqrt{R_r}$, and

$$V^{-1} F = \begin{bmatrix} 0 & \frac{\beta_{1y} s_y^0}{\sigma_y + \phi} & \frac{\beta_{2y} s_y^0}{\sigma_y + \phi} & 0 & \frac{\beta_{1o} s_y^0}{\sigma_y + \phi} & \frac{\beta_{2o} s_y^0}{\sigma_y + \phi} \\ \frac{p_y \sigma_y}{\gamma_y + \eta_y + \chi_y + \phi} & 0 & 0 & 0 & 0 & 0 \\ \frac{(1-p_y) \sigma_y}{\gamma_{1y} + \eta_{1y} + \phi} & 0 & 0 & 0 & 0 & 0 \\ 0 & \frac{\beta_{1y} \psi s_o^0}{\sigma_o + \phi} & \frac{\beta_{2y} \psi s_o^0}{\sigma_o + \phi} & 0 & \frac{\beta_{1o} \psi s_o^0}{\sigma_o + \phi} & \frac{\beta_{2o} \psi s_o^0}{\sigma_o + \phi} \\ 0 & 0 & 0 & \frac{p_o \sigma_o}{\gamma_o + \eta_o + \chi_o + \phi} & 0 & 0 \\ 0 & 0 & 0 & \frac{(1-p_o) \sigma_o}{\gamma_{1o} + \eta_{1o} + \phi} & 0 & 0 \end{bmatrix}.$$

This vector is

$$v_l = \left(\frac{\sigma_y + \phi}{\rho \beta_{2y} s_y^0} R_{ry}, \frac{\beta_{1y}}{\beta_{2y}}, 1, \frac{\sigma_o + \phi}{\rho \beta_{2y} s_o^0 \psi} R_{ro}, \frac{\beta_{1o}}{\beta_{2y}}, \frac{\beta_{2o}}{\beta_{2y}} \right),$$

and Lyapunov function L , constructed as $L = v_l V^{-1} x^T$, is

$$L = \frac{z_1}{\sigma_y + \phi} e_y + \frac{z_2}{\gamma_y + \eta_y + \chi_y + \phi} a_y + \frac{1}{\gamma_{1y} + \eta_{1y} + \phi} d_{1y} + \frac{z_4}{\sigma_o + \phi} e_o + \frac{z_5}{\gamma_o + \eta_o + \chi_o + \phi} a_o + \frac{z_6}{\gamma_{1o} + \eta_{1o} + \phi} d_{1o} \geq 0$$

always, and

$$\begin{aligned} \frac{d}{dt} L &= -(1-\rho) \frac{\sigma_y + \phi}{\rho \beta_{2y} s_y^0} R_{ry} e_y - (1-\rho) \frac{\sigma_o + \phi}{\rho \beta_{2y} s_o^0 \psi} R_{ro} e_o - \frac{1}{\rho \beta_{2y}} \lambda \left[\frac{R_{ry}}{s_y^0} (s_y^0 - \rho s_y) + \frac{R_{ro}}{s_o^0} (s_o^0 - \rho s_o) \right] \\ &+ e_y (\alpha_y d_{2y} + \alpha_o d_{2o}) + a_y (\alpha_y d_{2y} + \alpha_o d_{2o}) + d_{1y} (\alpha_y d_{2y} + \alpha_o d_{2o}) + \\ &e_o (\alpha_y d_{2y} + \alpha_o d_{2o}) + a_o (\alpha_y d_{2y} + \alpha_o d_{2o}) + d_{1o} (\alpha_y d_{2y} + \alpha_o d_{2o}) \leq 0 \end{aligned}$$

only if $\rho < 1$, $s_y^0 \geq s_y$, $s_o^0 \geq s_o$ and $\alpha_y = \alpha_o = 0$ ($(\sigma_j + \phi) / (\sigma_j + \phi s_j^0) > 1$).

Hence, the method proposed in [7] is valid only for $\alpha_y = \alpha_o = 0$, in which case P^0 is globally stable if $s_y^0 \geq s_y$, $s_o^0 \geq s_o$ and $\rho = \sqrt{R_r} \leq 1$.